Table S10. Results of serum biochemical tests following chronic toxicity tests in rabbits

Test	Date	Control	A549	AdE3-*IAI.3B*	Carrier cells (dose) low	moderate	high
TCHO	Pre	1.0±0.3	1.2±0.4	1.5±0.6*	1.3±0.4	1.3±0.4	1.2±0.5
(mmol/L)	Week 2	1.3±0.8	1.5±0.5	1.3±0.3	1.4±0.5	1.8±1.2	2.7±1.6*
	Week 4	1.1±0.2	1.3±0.4	1.4±0.3*	1.8±0.6*	2.3±1.3	2.4±1.1
	Week 8	1.4±0.4	1.7±0.1	2.3±0.6*	1.8±0.3	2.2±0.8	2.1±0.6*
TG	Pre	1.3±0.5	1.2±0.7	2.1±1.3	1.2±0.7	1.5±1.3	1.5±1.3
(mmol/L)	Week 2	1.7±0.6	2.0±0.7	1.9±0.7	1.9±0.5	1.9±0.7	3.4±1.9*
	Week 4	1.2±0.5	1.3±0.4	1.2±0.3	1.7±0.6	1.6±0.5	2.2±0.7*
	Week 8	1.5±0.3	1.0±0.4	1.4±0.6	1.1±0.4	1.3±0.1	1.4±0.4
BUN	Pre	8.3±1.2	8.3±2.0	7.9±1.7	7.2±2.4	8.8±1.8	8.4±2.1
(mmol/L)	Week 2	6.2±2.4	7.1±1.2	6.0±1.3	5.8±1.1	6.2±1.1	7.1±4.1
	Week 4	9.6±3.0	9.2±2.0	8.9±2.7	8.8±1.6	8.0±1.8	8.8±3.1
	Week 8	7.1±1.0	6.3±0.2	6.5±0.6	6.9±0.4	6.7±0.8	6.9±1.2
Creat	Pre	107±11	102±11	106±18	113±16	111±18	109±15
(μmol/L)	Week 2	93±10	89±12	98±10	95±18	91±9	70±27*
	Week 4	125±18	110±9	122±15	113±16	113±14	109±16
	Week 8	124±11	131±15	137±6	138±12	133±6	134±18
CK	Pre	2275±1037	2432±1246	2381±865	2334±899	2803±1347	2390±1223
(U/L)	Week 2	2701±1512	2826±1321	2100±816	3450±903	3355±1221	3262±1638
	Week 4	1582±508	1260±534	1574±700	2331±882*	1985±858*	1639±1323
	Week 8	922±154	1191±163	1357±511	1091±536	1591±499	1019±150
GLU	Pre	5.8±1.1	6.3±1.3	5.2±1.6	5.8±1.5	5.9±1.2	6.2±1.7
(μmol/L)	Week 2	5.0±1.0	5.4±1.2	5.2±0.7	5.1±1.1	5.3±1.1	5.7±1.3
	Week 4	5.9±0.9	5.9±1.0	5.7±1.5	7.3±2.5	6.1±1.9	6.3±1.3
	Week 8	6.2±0.7	5.9±0.5	6.0±0.2	5.7±0.8	5.9±0.9	6.2±1.2

TCHO, total cholesterol; TG, triglyceride; BUN, blood urea nitrogen; Creat, creatinine; CK, creatine kinase; GLU, glucose; Carrier cells, AdE3-*IAI.3B*-infected A549 cells; *, $P < 0.05$.

Cancer Science
Japanese Cancer Association JCA
Open Access

Characterization of common marmoset dysgerminoma-like tumor induced by the lentiviral expression of reprogramming factors

Saori Yamaguchi,[1,9] Tomotoshi Marumoto,[1,2,9] Takenobu Nii,[1] Hirotaka Kawano,[1] Jiyuan Liao,[1] Yoko Nagai,[1] Michiyo Okada,[1] Atsushi Takahashi,[3] Hiroyuki Inoue,[1,2] Erika Sasaki,[4] Hiroshi Fujii,[5] Shinji Okano,[5] Hayao Ebise,[6] Tetsuya Sato,[7] Mikita Suyama,[7] Hideyuki Okano,[8] Yoshie Miura[1] and Kenzaburo Tani[1,2]

[1]Division of Molecular and Clinical Genetics, Molecular and Clinical Genetics, Medical Institute of Bioregulation, Kyushu University, Fukuoka; [2]Department of Advanced Molecular and Cell Therapy, Kyushu University Hospital, Fukuoka; [3]Division of Translational Cancer Research Medical Institute of Bioregulation, Kyushu University, Fukuoka; [4]KEIO-RIKEN Research Center for Human Cognition, Keio University, Tokyo; [5]Division of Pathophysiological and Experimental Pathology, Department of Pathology, Kyushu University, Fukuoka; [6]Genomic Science Laboratories, Dainippon Sumitomo Pharma, Osaka; [7]Division of Bioinformatics, Medical Institute of Bioregulation, Kyushu University, Fukuoka; [8]Department of Physiology, Keio University, Tokyo, Japan

Key words

Common marmoset, FGFR, regenerating medicine, reprogramming factor, tumorigenesis

Correspondence

Kenzaburo Tani, Division of Molecular and Clinical Genetics, Department of Molecular Genetics, Medical Institute of Bioregulation, Kyushu University, 3-1-1 Maidashi, Higashi-ku, Fukuoka 812-8582 Japan.
Tel: +81-92-642-6434; Fax: +81-92-642-6444;
E-mail: taniken@bioreg.kyushu-u.ac.jp

[9]These authors contributed equally to this work.

Funding information

Project for Realization of Regenerative Medicine (08008010) and Kakenhi (23590465) from the Ministry of Education, Culture, Sports, Science and Technology (MEXT), Japan.

Received June 4, 2013; Revised January 14, 2014; Accepted February 5, 2014

Cancer Sci **105** (2014) 402–408

doi: 10.1111/cas.12367

Recent generation of induced pluripotent stem (iPSCs) has made a significant impact on the field of human regenerative medicine. Prior to the clinical application of iPSCs, testing of their safety and usefulness must be carried out using reliable animal models of various diseases. In order to generate iPSCs from common marmoset (CM; *Callithrix jacchus*), one of the most useful experimental animals, we have lentivirally transduced reprogramming factors, including POU5F1 (also known as OCT3/4), SOX2, KLF4, and c-MYC into CM fibroblasts. The cells formed round colonies expressing embryonic stem cell markers, however, they showed an abnormal karyotype denoted as 46, X, del(4q), +mar, and formed human dysgerminoma-like tumors in SCID mice, indicating that the transduction of reprogramming factors caused unexpected tumorigenesis of CM cells. Moreover, CM dysgerminoma-like tumors were highly sensitive to DNA-damaging agents, irradiation, and fibroblast growth factor receptor inhibitor, and their growth was dependent on c-MYC expression. These results indicate that DNA-damaging agents, irradiation, fibroblast growth factor receptor inhibitor, and c-MYC-targeted therapies might represent effective treatment strategies for unexpected tumors in patients receiving iPSC-based therapy.

The development of a technology to generate iPSCs from differentiated somatic cells by the transduction of a set of transcription factors, OSKM, made a significant impact in the field of basic research for regenerative medicine, in light of their potential use as a cell source for transplantation therapy for various kinds of incurable diseases.[1,2]

However, the low efficiency of iPSC generation, the need to induce their efficient differentiation into specific cell types, and the risk of tumor formation in recipients transplanted with iPSC-derived functional cells have hindered the clinical application of iPSCs.[3] The transduction of transcription factors, including the oncogene *c-MYC*, insertional mutation of the genome caused by virus vectors, and genomic instability due to the stress of long-term culture for reprogramming, might contribute to tumor development when iPSC-derived functional cells are applied to clinical practice.[4] Although the technology used to generate iPSCs has improved with the use of OSK without M,[5] non-viral vectors,[6] other molecules such as mRNA or miRNA,[7] and chemicals,[8] tumor formation in recipients remains a major concern.[9] Despite these issues, reprogramming factor-related tumor cells have not been well-characterized to date.

The CM (*Callithrix jacchus*) has several advantages as an experimental laboratory primate, including ease of handling, being inexpensive to house and feed, and a high reproductive rate.[10] Therefore, CM and CM-derived iPSCs represent useful experimental tools for testing the clinical utility of iPSC-based regenerative medicine *in vivo* and *in vitro*.

In this study, we attempted to generate iPSCs from CM fibroblasts, and inadvertently produced immature malignant tumor cells. We therefore analyzed the biological characteristics of these cells *in vitro* and *in vivo*. The results may provide useful information for the development of strategies to deal with tumors unexpectedly formed in patients treated with iPSC-based therapies.

Materials and Methods

Cell culture, induction of reprogramming, and proliferation assay. Common marmoset ARCs, CM ESCs, and iPS A cells derived from fetal liver cells (provided by Erika Sasaki, KEIO-REKEN Research Center for Human Cognition, Keio University, Tokyo, Japan) were maintained in DMEM/F12 (Sigma-Aldrich, St. Louis, MO, USA) containing 20% Knockout Serum Replacement (Gibco, Carlsbad, CA, USA), 0.1 mM non-essential amino acid (Gibco), 1 mM L-glutamine (Nacalai Tesque, Kyoto, Japan), 1% antibiotic–antimycotics (Nacalai Tesque), 0.4 mM 2-mercaptoethanol (Sigma Aldrich), and 0.12% sodium hydroxide (Nacalai Tesque). The CM DGs were maintained in DMEM/F12 containing 10% FBS at 37°C in a 5% humidified CO_2 atmosphere. Detailed descriptions of the cell culture, reprogramming method, and proliferation assay are provided in Figures 1 and 5.

Plasmids and lentiviral vector production. Human OCT3/4, SOX2, KLF4, or c-MYC was inserted into CSIV-CMV-MCS-IRES2-Venus lentiviral vectors (kindly provided by Hiroyuki Miyoshi, Riken, Tsukuba, Japan). Short hairpin RNAs targeting OCT3/4, SOX2, and c-MYC were obtained from Addgene (Cambridge, MA, USA), and shRNA targeting KLF4 was obtained from Applied Biological Materials (Richmond, BC, Canada). Lentiviruses were produced as previously described.[11]

Microarray analysis. Total RNA from AGM fibroblasts, ARCs, and iPS A cells were isolated using the RNeasy Mini Kit (Qiagen, Valencia, CA, USA). RNA was reverse-transcribed, biotin-labeled, and hybridized for 16 h to a marmoset genome oligonucleotide custom array Marmo2 (in preparation),[12] which was subsequently washed and stained in a Fluidics Station 450 (Affymetrix, Santa Clara, CA, USA) according to the manufacturer's instructions. Detailed protocols of microarray analysis are provided in Figures 2 and S5.

DNA-damaging treatments. The CM DGs were treated with 1 μg/mL MMC (Kyowa Hakko Kirin, Tokyo, Japan) or 10 μg /mL cisplatin (Sigma-Aldrich) for 1 h at 37°C. For irradiation, CM DGs were irradiated (20 Gy) using Gammacell 40 (Atomic Energy, Chalk River, Ontario, Canada). At 24 h after treatment, the cells were stained with propidium iodide (Nacalai Tesque), and the proportion of dead cells was analyzed as the sub-G_1 population by flow cytometry (FACSCalibur; BD Biosciences, San Jose, CA, USA).

Statistical analysis. Statistical analyses were carried out with the GraphPad Prism 5.0d software package (GraphPad Software, La Jolla, CA, USA). Statistical analyses were carried out using a two-tailed unpaired Student's *t*-test or one-way ANOVA followed by Tukey's multiple comparison test. $P < 0.05$ was considered statistically significant.

Additional information is provided in Supporting information.

Results

Characteristic of aorta-gonado-mesonephros fibroblast-derived colonies formed by transduction of reprogramming factors. To generate CM-derived iPSCs, reprogramming factors (OSKM) were transduced into AGM fibroblasts using lentiviral vectors (Fig. 1a). Then OSKM-transduced cells were transferred to mouse embryonic fibroblast feeder cells on day 7 post-infection, and cultured in medium for CM ESCs. We found that the cells formed sphere-like structures on day 17 post-infection (Fig. 1b). Moreover, these colonies showed AP activity

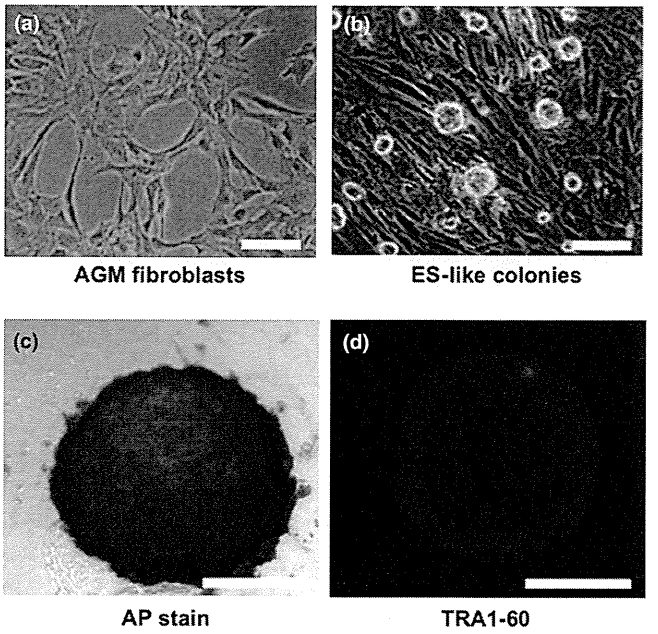

Fig. 1. Characterization of aorta-gonado-mesonephros (AGM) fibroblast-derived colonies formed by transduction of reprogramming factors. Representative phase-contrast images of (a) AGM fibroblasts and (b) abnormally reprogrammed cells (ARCs) forming round-shaped colonies. (c) Representative image showing expression of alkaline phosphatase (AP) activity in ARCs. (d) Immunocytochemical staining showing expression of TRA1-60 in ARCs. Bar = 100 μm.

(Fig. 1c), and expressed ESC markers such as TRA1-60, SALL1, LIN28, and DPPA4 (Figs 1d, S1). These results suggested that the reprogrammed AGM fibroblasts formed immature, round iPSC-like colonies.

Chromosome abnormality and tumor-forming ability in abnormally reprogrammed cells. Given that *KLF4* and *c-MYC* are well-known oncogenes,[13,14] transduction with OSKM transcription factors may cause cell transformation and chromosome instability.[15] We carried out karyotype analysis of the colony-forming cells to determine if OSKM-transduced AGM fibroblasts exhibited chromosome instability. The normal karyotype of CM cells is 44 autosomes and two sex chromosomes (46, XX or 46, XY).[16] However, the round colony-forming cells contained 44 autosomes, one X chromosome, and an abnormal marker chromosome (mar), with deletions of chromosome 4q, and were therefore denoted as 46, X, del (4q), +mar (Fig. 2a, right panel). The karyotype of the parental AGM fibroblasts was 46, X, +mar (Fig. 2a, left panel). These results suggested that the reprogramming stress induced by OSKM might have caused the deletion of 4q, although the possibility that the stress of long-term *in vitro* culture might have resulted in chromosome instability could not be excluded. These colony-forming cells were named ARCs.

To examine the ability of ARCs to differentiate into three germ layers like ESCs, we carried out an *in vitro* differentiation assay based on the protocol for human ESC differentiation.[17,18] Unlike human ESCs, ARCs did not differentiate into neural progenitors, cardiomyocytes, or hepatic cells (Fig. S2, Video S1).

We carried out *in vivo* differentiation assays by injecting ARCs into the testes of SCID mice. Approximately 6 weeks after injection, 11 of 18 mice injected with ARCs showed

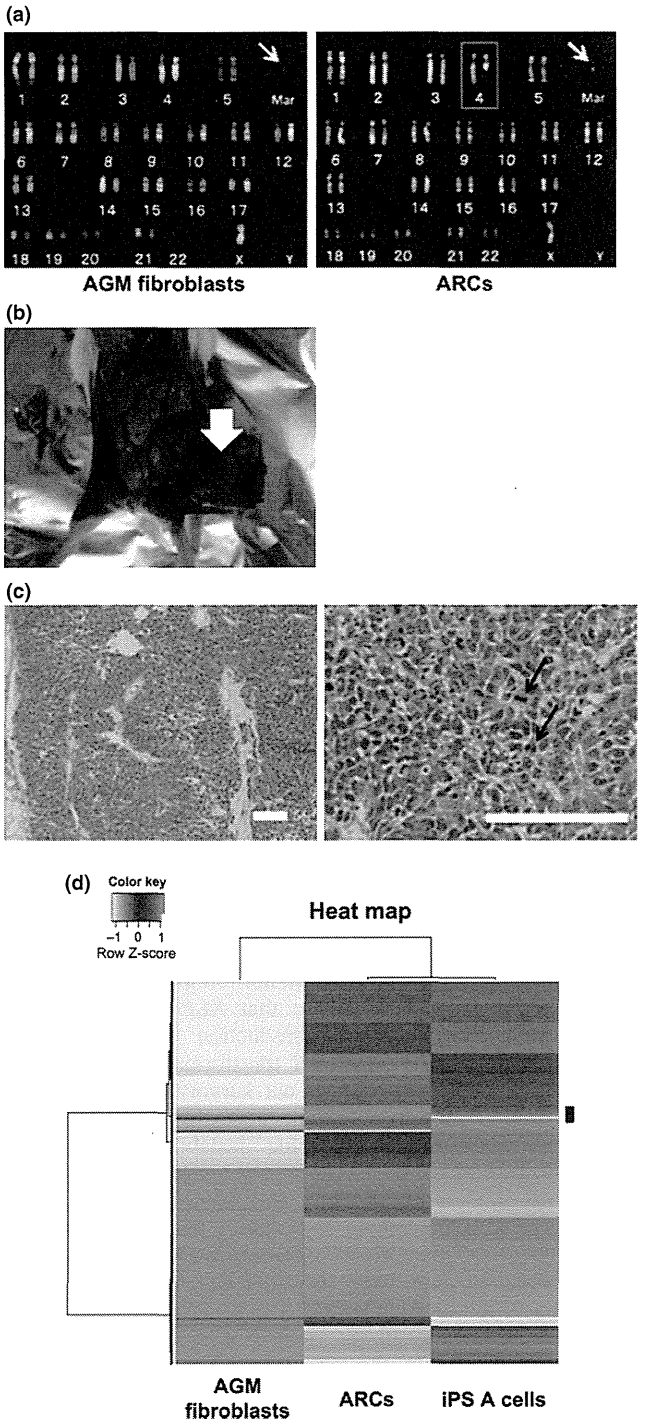

Fig. 2. Chromosome abnormality and tumor-forming ability in abnormally reprogrammed cells (ARCs). (a) Karyotype analyses of aorta-gonado-mesonephros (AGM) fibroblasts (left panel) and ARCs (right panel). Arrows indicate marker chromosome. Blue outline indicates the deletion of 4q. Mar, marker chromosome. (b) Representative photograph of dysgerminoma-like tumor (arrow) formed by transplantation of ARCs into SCID mice. (c) Hematoxylin-eosin staining of dysgerminoma-like tumor tissues. Arrows in right panel indicate mitotic figures in tumor cells. Bar = 100 μm. (d) Microarray analysis. Gene expressions in AGM fibroblasts, ARCs, and normal induced pluripotent stem (iPS) A cells were analyzed by unsupervised hierarchical clustering. A heat map using probes showing differential expression levels in each cell line is shown. Red indicates upregulation; green indicates downregulation. The black bar on the right side of the heat map shows candidate differentially expressed probes in ARCs.

tumor formation (Fig. 2b), whereas no mice injected with AGM fibroblasts showed tumor formation (0/3, data not shown). Staining with H&E revealed that the tumors were relatively homogenous, with high cellular density, necrosis, and pleomorphism, indicating their malignant phenotype (Fig. 2c). In addition, tumors were composed of nests and sheets of uniform round or polygonal cells with abundant, clear to faintly eosinophilic cytoplasm with well-demarcated cytoplasmic borders and a delicate network of thin-walled blood vessels in the tumor nests (Fig. 2c, right panel). Furthermore, immunohistochemical analyses revealed that the tumor cells were focally and weakly immunopositive for vimentin, and immunonegative for the differentiation markers cytokeratin, S100, desmin, α-smooth muscle actin, and neuron-specific enolase (data not shown). Tumor tissues also expressed c-KIT, but not CD30 or CD45 (Fig. S3). These molecular expression profiles implied that the tumor was equivalent to human malignant dysgerminoma, rather than other types of immature tumors such as embryonal carcinoma, yolk sac tumor, or teratoma.[19,20] The tumor was named CM DG.

We next carried out soft agar assays to determine if ARCs were transformed and showed anchorage-independent growth as a result of ectopic expression of reprogramming factors. The ARCs were cultured in 0.5% agarose-containing medium for 20 days, and the number of colonies was counted. The ARCs formed many colonies, compared with parental AGM fibroblasts (Fig. S4a and data not shown). These results strongly suggested that ARCs were transformed during reprogramming, and acquired the capacity for anchorage-independent growth. To clarify the contribution of reprogramming factors that could transform AGM fibroblasts, we transduced various combinations of these factors into AGM fibroblasts, and examined if the transduced cells were transformed by the colony formation assay on mouse embryonic fibroblasts, AP staining assay, and soft agar assay. The iPSC-like colonies were found in OSKM- and OSM-transduced cells (OSKM, 30 ± 3/5000; OSM, 6 ± 0/5000), but they were not found at all when OSK, OS, OM, SM, O, S, K, or M were transduced (Fig. S4b). AP activity was found in both OSKM- and OSM-transduced cells, although OSM-transduced cells showed weaker AP activity than OSKM-transduced cells (Fig. S4c). In soft agar assay, the anchorage-independent growth was found in both OSKM- and OSM-transduced cells (Fig. S4d; OSKM, 160 ± 23/1000; OSM, 163 ± 10/1000). These results indicated that the simultaneous expression of OCT3/4, SOX2, and c-MYC was at least required for the transformation of AGM fibroblasts, while KLF4 did not play a major role in the transformation of AGM fibroblasts.

Tomioka *et al.* reported the establishment of CM iPSCs (iPS A cells) showing normal karyotype.[12] To characterize the gene expression in ARCs, we carried out microarray analyses using mRNA from ARCs, iPS A cells, and AGM fibroblasts. According to the clustering pattern and the heat map, 171 probes that showed higher expression levels in ARCs as compared to other cells were selected as candidate differentially expressed genes in ARCs (Fig. 2d). Moreover, we focused on the genes specifically highly expressed in ARCs compared to those in iPS A cells, and the top seven genes highly expressed in ARCs were selected (*ZFHX4*, *PCDH19*, *NFIX*, *HOXC8*, *STMN2*, *SERPINA3*, and *CXORF67*). Then we validated these data by semiquantitative RT-PCR analyses, and five genes (*ZFHX4*, *NFIX*, *HOXC8*, *STMN2*, and *CXORF67*) were confirmed to be more expressed in ARCs than those in controls (Fig. S5). The high expression of these five genes might be characteristics of ARCs.

Characteristic of CM DGs. We then surgically removed CM DGs and cultured them *in vitro* to examine their biological characteristics. The CM DGs could grow infinitely in a semi-floating state in the culture dish, and showed continuous expression of Venus fluorescent protein (Fig. 3a,b). We generated five CM DG cell lines (CMY401, CMY402a, CMY402b, CMY403a, and CMY403b) from five independent tumors formed by the injection of ARCs into SCID mice, and found that all four transduced reprogramming factors were integrated into their genomes (Fig. S6a). Both endogenous and exogenous reprogramming factors were expressed in these cell lines (Fig. 3c,d).

Effects of DNA-damaging agents and irradiation on CM DGs. Dysgerminomas are generally sensitive to cisplatin and irradiation.[21,22] We therefore examined the effects of DNA-damaging agents such as MMC and cisplatin on CM DGs. Three CM DG cell lines (CMY402a, CMY402b, and CMY403a) were treated with MMC for 1 h, and the proportion of dead cells was analyzed by flow cytometry at 24 h after treatment. The percentage of cells with a sub-G_1 DNA content was taken as a measure of dead cells in the population. The proportion of dead cells in MMC-treated CM DG cultures was significantly higher than that in controls (MMC-treated AGM fibroblasts) (Figs 4a, S7). Similar results were obtained when these three cell lines were treated with cisplatin or irradiation (Figs 4b,c, S8, S9). These results suggested that CM DGs were

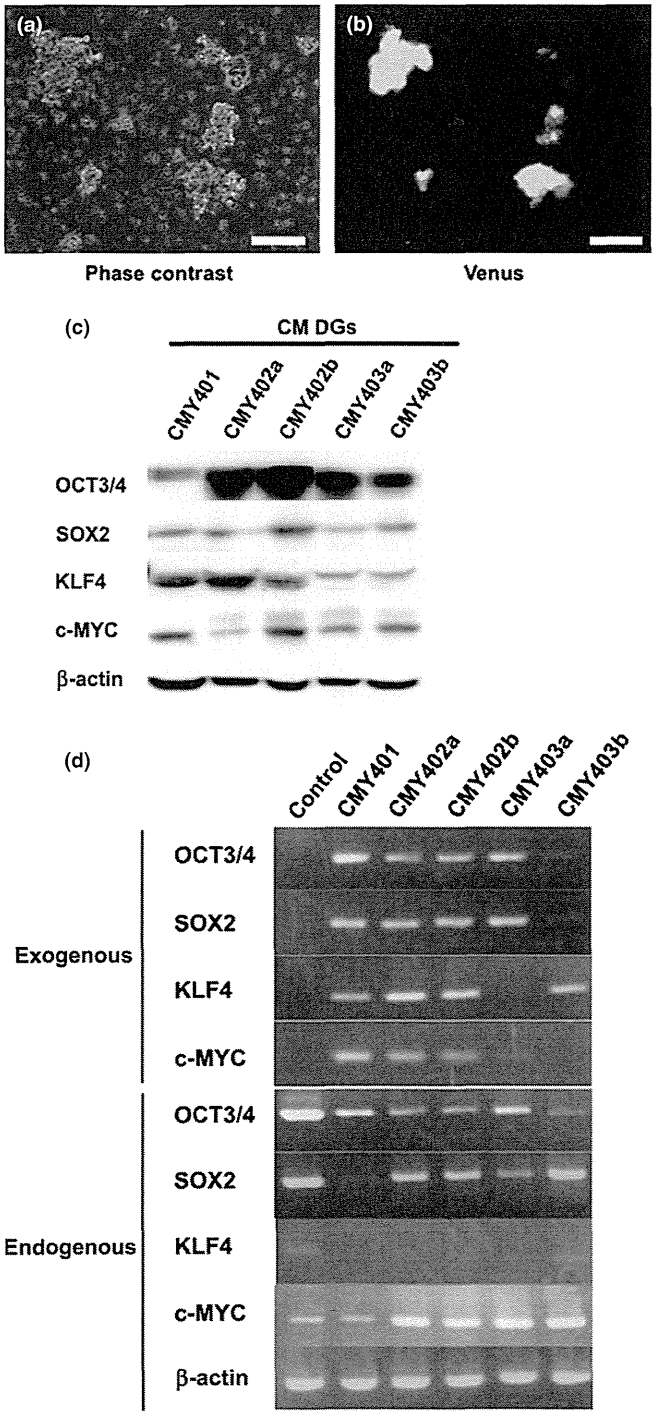

Fig. 3. Characterization of common marmoset dysgerminoma-like (CM DG) cells in culture. (a) Representative phase-contrast image of CM DGs. (b) Immunofluorescent image of Venus expression in CM DGs. Bar = 100 μm. (c) Western blot analysis showing expression of reprogramming factors in CM DG cell lines. (d) RT-PCR analysis showing the expression of endogenous or exogenous reprogramming factors in CM DGs. Cj11 (CM embryonic stem cell line) was used as control.

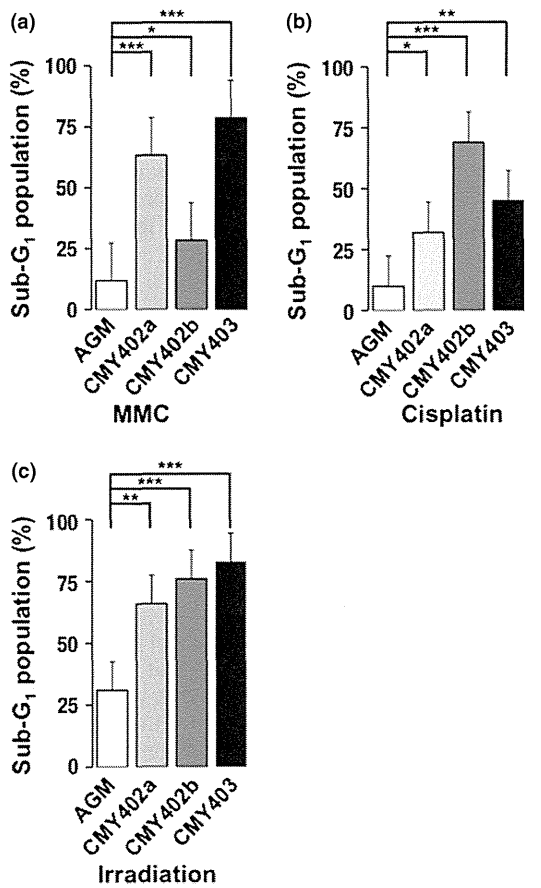

Fig. 4. Effects of DNA-damaging agents and irradiation on common marmoset dysgerminoma-like cells (CM DGs). The cells were treated with (a) mitomycin C (MMC), (b) cisplatin, or (c) irradiation, and the proportions of sub-G_1 populations in aorta-gonado-mesonephros (AGM) fibroblasts or CM DG cell lines were analyzed by FACS. Results are shown as means ± SD. $^*P < 0.05$; $^{**}P < 0.01$; $^{***}P < 0.001$.

more sensitive to DNA damage than their parental AGM fibroblasts.

We carried out inverse PCR analyses to identify the integration sites of the lentiviral vectors expressing reprogramming factors in CM DGs. OCT 3/4-, SOX2-, KLF4-, and c-MYC-expressing lentiviral vectors were integrated into 5, 12, 5, and 9 genomic sites, respectively (Fig. S6b, Table S1). The possibility that multiple integrations of lentiviral vectors into the genome caused chromosome instability, leading to the formation of CM DGs, could therefore not be excluded.

Dependence of CM DGs growth on c-MYC and bFGF signalings. To address the question of whether proliferation of CM DGs was dependent on reprogramming factors, we observed the proliferation rate after suppression of each reprogramming factor by shRNA (Fig. S10). Suppression of c-MYC or all four reprogramming factors greatly inhibited the proliferation of CM DGs, indicating that the growth of CM DGs was highly dependent on c-MYC (Fig. 5a).

The proliferation of human ESCs is known to be promoted by bFGF signaling.[23] We examined the possibility that the growth of CM DGs might also be enhanced by bFGF signaling by analyzing the proliferation of CM DGs cultured in medium with or without bFGF. The growth of CM DGs was highly dependent on bFGF (Fig. 5b). Consistent with these results, BGJ398, an inhibitor for FGFR 1 to 4, remarkably inhibited the growth of CM DGs in a dose-dependent manner (Fig. 5c). Moreover, FACS analyses revealed that the sub-G_1 population, representing dead cells, was increased in the presence of BGJ398 (Fig. S11). It should be emphasized that the IC_{50} of BGJ398 (59 nM) was lower for CM DGs than for their parental AGM fibroblasts and control CM skin fibroblasts (Fig. 5d), indicating higher sensitivity of CM DGs. These results suggested that the growth of CM DGs was dependent on bFGF signaling, and therefore FGFR inhibitor could be used to control the growth of the reprogramming factor-induced tumor.

Discussion

In this study we investigated the characteristics of ARCs and CM DGs generated in the reprogramming process of CM AGM fibroblasts by Yamanaka factors.

A normal iPSC line of iPS A cells, showed the expression of ES markers, pluripotency, and flattened morphology, like human iPSCs.[20] In contrast, ARCs showed sphere-like structures, like mouse iPSCs.[1] This morphological difference between iPS A cells and ARCs might be useful to select "true" iPSCs derived from CM, although the underlying molecular mechanisms responsible for this morphological difference remain unknown.

We found, by microarray analyses, that the gene expression pattern in ARCs was more similar to that in iPS A cells than that in AGM fibroblasts, suggesting that reprogramming processes have been done in ARCs by the transduction of reprogramming factors. We also found that genes such as *ZFHX4*, *NFIX*, *HOXC8*, *STMN2*, and *CXORF67* were highly expressed in ARCs. It should be noted that, among these, *HOXC8* is known to be a transcriptional factor related to tumorigenesis.[24] Therefore, these candidates of markers might be useful to predict the tumorigenic potential of iPSCs. Further evaluation is required to confirm our hypothesis.

The original AGM fibroblasts had an abnormal marker chromosome (mar; Fig. 2a, left panel). Although tumor formation was not evident caused in SCID mice (data not shown), this chromosome instability might also be one of the inducers of

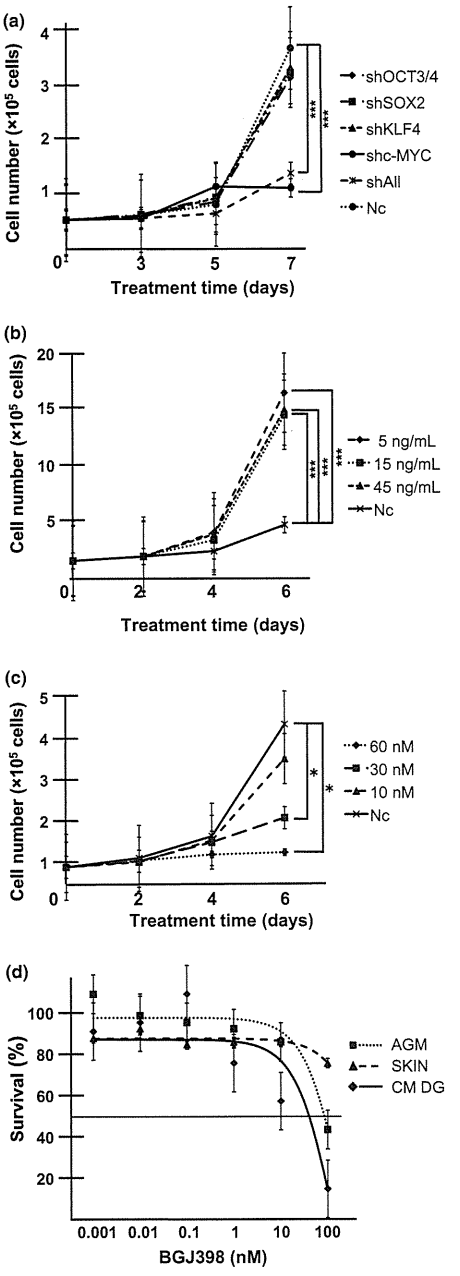

Fig. 5. Dependence of common marmoset dysgerminoma-like (CM DG) cell growth on c-MYC and basic fibroblast growth factor (bFGF) signaling. (a) Inhibition of CM DG growth by knockdown of c-MYC. Cells (3×10^4) were seeded on 24-well plates and transduced with shRNA targeting OCT3/4, SOX2, KLF4, c-MYC, or all reprogramming factors (shAll). Cell growth curves were analyzed by cell counts at the indicated time points. Results are shown as means ± SD. ***$P < 0.001$. Nc, negative control (mock vector). (b) Growth rate of CM DGs was promoted by the addition of bFGF. Cells were cultured in the presence or absence (Nc) of bFGF. Cell numbers were counted at the indicated time points. Results are shown as means ± SD. ***$P < 0.001$. (c) FGFR inhibitor suppressed CM DG growth. Cells were cultured in the presence or absence (Nc) of the FGFR1-4 inhibitor BGJ398; bFGF was added at 5 ng/mL. Cell numbers were counted at the indicated time points. Results are shown as means ± SD. *$P < 0.05$. (d) CM DGs, aorta-gonado-mesonephros fibroblasts (AGM), and CM skin fibroblasts (SKIN) were treated with different concentrations of BGJ398 for 3 days, and the growth-inhibitory effects were analyzed by MTS assay. The IC_{50} for CM DGs was lower than those for parental AGM fibroblasts and control CM skin fibroblasts. Results are shown as means ± SD.

carcinogenesis during the reprogramming process. Thus, needless to say, to generate "safe" iPSCs, validation of the karyotype of the original cells is needed. Moreover, ARCs lost chromosome 4q and X or Y, and possessed an abnormal marker chromosome (mar). Various tumor suppressors including human tumor suppressor gene 1, large tumor suppressor 1 and P36 transformed follicular lymphoma gene have been identified on chromosome 4q in CM cells (Table S2), suggesting that loss of these tumor suppressors might have induced the transformation of CM AGM fibroblasts during reprogramming, although the possibility that translocation of chromosome 4q occurred during the reprogramming process caused the transformation of cells could not be excluded.

It is also possible that the continuous activation of ectopically-transduced transcription factors, including the oncogene *c-MYC*, might have contributed to cell transformation, as described previously.[25,26] Indeed, CM DGs overexpressed c-MYC, and their growth was highly dependent on c-MYC expression, suggesting that downregulation of c-MYC might represent a possible strategy for inhibiting the growth of reprogramming factor-related tumors.

Insertional mutation caused by the integration of lentiviral vectors into the genome might also have promoted cell transformation. Lentiviral vectors expressing reprogramming factors were integrated into at least 31 different genomic sites in CM DGs, some of which were in the vicinity of protein-encoding genes. Moreover, the expression of reprogramming factors transduced by lentiviral vectors continued for over a year in ARCs (data not shown). A safer method, without genome integration, is therefore required for the delivery of reprogramming factors to somatic cells to generate iPSCs applicable for transplantation therapies. Although Sendai virus vectors or transfection of DNA or mRNA may be safer methods,[27] these are lengthy processes that can take more than 1 month to obtain iPSCs,[28] which could also cause stress and lead to genomic instability and subsequent tumor formation. More sophisticated, safer, and more rapid methods of reprogramming might be desirable.

Common marmoset DGs resembled human dysgerminomas in terms of both their pathology and sensitivity to irradiation and DNA-damaging agents.[21,22] In addition, the growth of CM DGs was significantly inhibited by an FGFR1-4 inhibitor. Therefore irradiation, chemotherapy, and FGFR1-4 inhibitors might be effective strategies for controlling human dysgerminomas, and also for tumors that develop in patients treated with iPSC-based therapies.

Acknowledgments

We thank Hiroyuki Miyoshi (Riken, Tsukuba, Japan) for providing lentiviral vectors, Norihiko Kinoshita (Kyushu University, Fukuoka, Japan) and the Laboratory for Technical Support (Medical Institute of Bioregulation, Kyushu University) for their technical assistance, Michiko Ushijima for administrative assistance, and members of Prof. Kenzaburo Tani's laboratory for constructive criticisms. This work was supported by grants from the Project for Realization of Regenerative Medicine (K.T., 08008010) and Kakenhi (T.M., 23590465) from the Ministry of Education, Culture, Sports, Science and Technology, Japan.

Disclosure Statement

The authors have no conflicts of interest.

Abbreviations

AGM	aorta-gonado-mesonephros
AP	alkaline phosphatase
ARC	abnormally reprogrammed cell
bFGF	basic fibroblast growth factor
CM	common marmoset
DG	human dysgerminoma-like cell
ESC	embryonic stem cell
FGFR	fibroblast growth factor receptor
iPSC	induced pluripotent stem cell
K	KLF4
M	c-MYC
MMC	mitomycin C
O	OCT3/4
S	SOX2

References

1 Takahashi K, Yamanaka S. Induction of pluripotent stem cells from mouse embryonic and adult fibroblast cultures by defined factors. *Cell* 2006; **126**: 663–76.
2 Okita K, Yamanaka S. Induced pluripotent stem cells: opportunities and challenges. *Philos Trans R Soc Lond B Biol Sci* 2011; **366**: 2198–207.
3 Okita K, Ichisaka T, Yamanaka S. Generation of germline-competent induced pluripotent stem cells. *Nature* 2007; **448**: 313–U1.
4 Ohm JE, Mali P, Van Neste L *et al.* Cancer-related epigenome changes associated with reprogramming to induced pluripotent stem cells. *Cancer Res* 2010; **70**: 7662–73.
5 Wernig M, Meissner A, Cassady JP, Jaenisch R. c-Myc is dispensable for direct reprogramming of mouse fibroblasts. *Cell Stem Cell* 2008; **2**: 10–2.
6 Okita K, Nakagawa M, Hong HJ, Ichisaka T, Yamanaka S. Generation of mouse induced pluripotent stem cells without viral vectors. *Science* 2008; **322**: 949–53.
7 Judson RL, Babiarz JE, Venere M, Blelloch R. Embryonic stem cell-specific microRNAs promote induced pluripotency. *Nat Biotechnol* 2009; **27**: 459–61.
8 Lin TX, Ambasudhan R, Yuan X *et al.* A chemical platform for improved induction of human iPSCs. *Nat Methods* 2009; **6**: 805–U24.
9 Madonna R. Human-induced pluripotent stem cells. in quest of clinical applications. *Mol Biotechnol* 2012; **52**: 193–203.
10 Lunn SF. Systems for collection of urine in the captive common marmoset, *Callithrix-Jacchus*. *Lab Anim* 1989; **23**: 353–6.
11 Marumoto T, Tashiro A, Friedmann-Morvinski D *et al.* Development of a novel mouse glioma model using lentiviral vectors. *Nat Med* 2009; **15**: 110–6.
12 Tomioka I, Maeda T, Shimada H *et al.* Generating induced pluripotent stem cells from common marmoset (*Callithrix jacchus*) fetal liver cells using defined factors, including Lin28. *Genes Cells* 2010; **15**: 959–69.
13 Foster KW, Frost AR, McKie-Bell P *et al.* Increase of GKLF messenger RNA and protein expression during progression of breast cancer. *Cancer Res* 2000; **60**: 6488–95.
14 Gustafson WC, Weiss WA. Myc proteins as therapeutic targets. *Oncogene* 2010; **29**: 1249–59.
15 Vogelstein B. Genetic instabilities in human cancers. *Biophys J* 1999; **76**: A135–A.
16 Sasaki E, Hanazawa K, Kurita R *et al.* Establishment of novel embryonic stem cell lines derived from the common marmoset (*Callithrix jacchus*). *Stem Cells* 2005; **23**: 1304–13.
17 Li XJ, Du ZW, Zarnowska ED *et al.* Specification of motoneurons from human embryonic stem cells. *Nat Biotechnol* 2005; **23**: 215–21.
18 Liao JY, Marumoto T, Yamaguchi S *et al.* Inhibition of PTEN tumor suppressor promotes the generation of induced pluripotent stem cells. *Mol Ther* 2013; **21**: 1242–50.
19 Tumor of the ovary, Maldeveloped Gonads, Fallopian tube, and Broad Ligament., 1998; 239–65.
20 Ulbright TM. Germ cell tumors of the gonads: a selective review emphasizing problems in differential diagnosis, newly appreciated, and controversial issues. *Mod Pathol* 2005; **18** (Suppl 2): S61–79.

21 Brewer M, Gershenson DM, Herzog CE, Mitchell MF, Silva EG, Wharton JT. Outcome and reproductive function after chemotherapy for ovarian dysgerminoma. *J Clin Oncol* 1999; **17**: 2670–5.
22 Thoeny RH, Dockerty MB, Hunt AB, Childs DS Jr. A study of ovarian dysgerminoma with emphasis on the role of radiation therapy. *Surg Gynecol Obstet* 1961; **113**: 692–8.
23 Bendall SC, Stewart MH, Menendez P *et al.* IGF and FGF cooperatively establish the regulatory stem cell niche of pluripotent human cells in vitro. *Nature* 2007; **448**: 1015–U3.
24 Li Y. HOXC8-dependent cadherin 11 expression facilitates breast cancer cell migration through trio and rac. *Genes Cancer* 2011; **2**: 880–8.
25 Nakagawa M, Koyanagi M, Tanabe K *et al.* Generation of induced pluripotent stem cells without Myc from mouse and human fibroblasts. *Nat Biotechnol* 2008; **26**: 101–6.
26 Gordan JD, Thompson CB, Simon MC. HIF and c-Myc: sibling rivals for control of cancer cell metabolism and proliferation. *Cancer Cell* 2007; **12**: 108–13.
27 Seki T, Yuasa S, Fukuda K. Derivation of induced pluripotent stem cells from human peripheral circulating T cells. *Curr Protoc Stem Cell Biol* 2011; 11–14. Chapter 4: Unit4A.3.
28 Buganim Y, Faddah DA, Cheng AW *et al.* Single-cell expression analyses during cellular reprogramming reveal an early stochastic and a late hierarchic phase. *Cell* 2012; **150**: 1209–22.

Supporting Information

Additional supporting information may be found in the online version of this article:

Fig. S1. Expression of embryonic stem cell (ESC) markers in abnormally reprogrammed cells (ARCs).

Fig. S2. Impaired differentiation of abnormally reprogrammed cells (ARCs).

Fig. S3. Expression of c-KIT, CD30, and CD45 in common marmoset dysgerminoma-like cells.

Fig. S4. Colony formation of aorta-gonado-mesonephros fibroblasts by the transduction of OCT3/4, SOX2, KLF4, and c-MYC (OSKM) and OSM.

Fig. S5. Validation of genes showing upregulation in abnormally reprogrammed cells (ARCs) compared to normal induced pluripotent stem (iPS) A cells in microarray analysis.

Fig. S6. Integration of reprogramming genes into the genome of common marmoset dysgerminoma-like cells (CM DGs).

Fig. S7. Fluorescence-activated cell sorter analyses to reveal effects of mitomycin C treatment on common marmoset dysgerminoma-like cell lines.

Fig. S8. Fluorescence-activated cell sorter analyses to reveal effects of cisplatin treatment on common marmoset dysgerminoma-like cell lines.

Fig. S9. Fluorescence-activated cell sorter analyses to reveal effects of irradiation on common marmoset dysgerminoma-like cell lines.

Fig. S10. Knockdown of OCT3/4, SOX2, KLF4, or c-MYC by shRNA in common marmoset dysgerminoma-like cell lines.

Fig. S11. Induction of cell death in common marmoset dysgerminoma-like cells by BGJ398.

Table S1. Lentiviral vector integration sites in common marmoset (CM) dysgerminoma-like cells.

Table S2. Human homologs of candidate tumor suppressors located on chromosome 4q in common marmoset (CM).

Video S1. *In vitro* differentiation assay to assess the ability of abnormally reprogrammed cells to differentiate into cardiomyocytes.

Data S1. Materials and Methods.

FEBS Open Bio 4 (2014) 213–219

FEBS openbio

journal homepage: www.elsevier.com/locate/febsopenbio

Analysis of essential pathways for self-renewal in common marmoset embryonic stem cells

Takenobu Nii [a,1], Tomotoshi Marumoto [a,b,1], Hirotaka Kawano [a], Saori Yamaguchi [a], Jiyuan Liao [a], Michiyo Okada [a], Erika Sasaki [c,d], Yoshie Miura [a], Kenzaburo Tani [a,b,*]

[a] Division of Molecular and Clinical Genetics, Medical Institute of Bioregulation, Kyushu University, 3-1-1, Maidashi, Higashi-ku, Fukuoka 812-8582, Japan
[b] Department of Advanced Molecular and Cell Therapy, Kyushu University Hospital, 3-1-1, Maidashi, Higashi-ku, Fukuoka 812-8582, Japan
[c] Central Institute for Experimental Animals, Kawasaki, Kanagawa 216-0001, Japan
[d] Keio Advanced Research Center, Keio University School of Medicine, Tokyo 160-8582, Japan

ARTICLE INFO

Article history:
Received 21 November 2013
Revised 12 February 2014
Accepted 12 February 2014

Keywords:
Embryonic stem cells
Common marmoset
bFGF
TGFβ
Self-renewal

ABSTRACT

Common marmoset (CM) is widely recognized as a useful non-human primate for disease modeling and preclinical studies. Thus, embryonic stem cells (ESCs) derived from CM have potential as an appropriate cell source to test human regenerative medicine using human ESCs. CM ESCs have been established by us and other groups, and can be cultured *in vitro*. However, the growth factors and downstream pathways for self-renewal of CM ESCs are largely unknown. In this study, we found that basic fibroblast growth factor (bFGF) rather than leukemia inhibitory factor (LIF) promoted CM ESC self-renewal via the activation of phosphatidylinositol-3-kinase (PI3K)-protein kinase B (AKT) pathway on mouse embryonic fibroblast (MEF) feeders. Moreover, bFGF and transforming growth factor β (TGFβ) signaling pathways cooperatively maintained the undifferentiated state of CM ESCs under feeder-free condition. Our findings may improve the culture techniques of CM ESCs and facilitate their use as a preclinical experimental resource for human regenerative medicine.

1. Introduction

Human regenerative medicine, including transplantation of various functional cells differentiated from embryonic stem cells (ESCs) or induced pluripotent stem cells (iPSCs), is considered to have great potential for treating various incurable diseases, and has thus attracted much public attention. However, preclinical studies using animal disease models are required to evaluate the efficacy and safety of ESC/iPSC-derived cells prior to their clinical application. Common marmoset (CM, *Callithrixjacchus*) has recently been recognized as a useful non-human primate for such studies, because of its small size, high reproductive capacity, and genetic similarity to humans [1].

Understanding the molecular mechanisms governing the self-renewal of ESCs is important for the development of technologies to differentiate them into functional cells. Although both human and mouse ESCs are able to self-renew on feeder cells in vitro, their growth factor requirements for self-renewal are different. Basic fibroblast growth factor (bFGF), which activates phosphatidylinositol-3-kinase (PI3K)-protein kinase B (AKT) [2,3] and mitogen-activated protein/extracellular signal-regulated kinase kinase (MEK)-extracellular signal-regulated kinase (ERK) pathways [2–8], and transforming growth factor β (TGFβ) leading to the activation of mothers against decapentaplegic homolog 2/3 (SMAD2/3) [2,6–11], maintain the self-renewal of human ESCs and mouse epiblast stem cells (EpiSCs). Conversely, in mouse ESCs, leukemia inhibitory factor (LIF), which activates janus kinase (JAK)-signal transducer and activator of transcription 3 (STAT3) and PI3K-AKT pathways, is known to play important roles in maintaining self-renewal [12–14].

Abbreviations: AKT, protein kinase B; bFGF, basic fibroblast growth factor; CM, common marmoset; EB, embryoid body; EpiSCs, epiblast stem cells; ERK, extracellular signal-regulated kinase; ESCs, embryonic stem cells; FCM, flow cytometry; iPSCs, induced pluripotent stem cells; JAK, janus kinase; KSR, knockout serum replacement; LIF, leukemia inhibitory factor; MEFs, mouse embryonic fibroblasts; MEK, mitogen-activated protein/extracellular signal-regulated kinase kinase; PI3K, phosphatidylinositol-3-kinase; RT-PCR, reverse transcription-polymerase chain reaction; SMAD2/3, mothers against decapentaplegic homolog 2/3; STAT3, signal transducer and activator of transcription 3; TGFβ, transforming growth factor β

* Corresponding author at: Division of Molecular and Clinical Genetics, Medical Institute of Bioregulation, Kyushu University, 3-1-1, Maidashi, Higashi-ku, Fukuoka 812-8582, Japan. Tel.: +81 92 642 6434; fax: +81 92 642 6444.
E-mail address: taniken@bioreg.kyushu-u.ac.jp (K. Tani).

[1] The first two authors contributed equally to this work.

http://dx.doi.org/10.1016/j.fob.2014.02.007
2211-5463/

ESCs derived from CM have been established by us and others [15–17]. However, the growth factors used in the culture medium are different among reports [15,17–21]. Thus, the most appropriate growth factor and its downstream pathway for maintaining the self-renewal of CM ESCs still remain to be determined.

In the present study, we characterized two CM ESC cell lines, Cj11 and CM40, and found that CM ESCs were more similar to human ESCs rather than mouse ESCs in terms of their growth factor requirement and molecular signaling pathways for self-renewal.

2. Materials and methods

2.1. CM ESC culture on mouse embryonic fibroblasts (MEFs)

CM ESC lines, CM40 and Cj11, were maintained in CM ESC medium as described before [15] with or without 1:1000 LIF (Wako, Osaka, Japan), 5 ng/ml bFGF (PeproTech, NJ, USA), 5 μM PD0325901 (MEK inhibitor, Wako) or 10 μM LY294002 (PI3K inhibitor, Santa Cruz Biotechnology, CA, USA). CM40 cell line was established in our laboratory [15], and Cj11 cell line was obtained from WiCell Research Institute [16]. MEFs were prepared from 13.5 dpc embryos from ICR mice (Charles River, Japan) using established procedures [22].

2.2. CM ESC culture under feeder-free conditions

CM40 and Cj11 ESC lines were cultured on Matrigel (BD Biosciences, CA, USA)-coated dishes in Essential 8 medium (Life Technologies, NY, USA) or Essential 6 medium (Life Technologies) with or without 1:1000 LIF (Wako), 100 ng/ml bFGF (PeproTech), 2 ng/ml TGFβ (PeproTech), 5 μM PD0325901 (MEK inhibitor, Wako), 10 μM LY294002 (Santa Cruz Biotechnology).

2.3. CM ESC differentiation

Undifferentiated ESCs were detached from the feeder cells by treatment with 0.25% trypsin (NacalaiTesque, Kyoto, Japan) for 1 min. The collected colonies were processed for embryoid body (EB) formation assay in CM ESC medium on low cell-binding 12-well plates (Nalge Nunc International KK, Japan) for 4 or 8 days. Detailed protocols to differentiate CM ESCs into three germ layers are described in "Supplementary Materials and Methods".

2.4. Immunocytochemistry

Cells were fixed in 4% paraformaldehyde (PFA)/phosphate-buffered saline (PBS) (NacalaiTesque), permeabilized with 0.3% Triton X-100/PBS, blocked with staining buffer (2% fetal bovine serum (FBS)/PBS). The primary antibodies used are shown in Supplementary Table 1. Nuclei were counterstained with DAPI. Images were obtained under a fluorescence microscope (Axiovert 135M; Carl Zeiss, Germany, or BZ-9000; Keyence) and then analyzed by Axiovert software (Carl Zeiss) or BZ-Analyzer software (Keyence).

2.5. Flow cytometry (FCM)

CM ESCs were fixed in 4% PFA/PBS, permeabilized with 0.3% Triton X-100/PBS, blocked with staining buffer (2% FBS/PBS), and then incubated with an anti-OCT3/4 antibody (Santa Cruz Biotechnology, sc-5279 or sc-8628). The cells were detected on a FACSVerse flow cytometer (Becton Dickinson, USA), followed by data analysis using FlowJo software (Tomy Digital Biology, Japan).

2.6. Reverse transcription-polymerase chain reaction (RT-PCR)

Total RNA was isolated using an RNeasy Mini Kit (Qiagen, USA), and cDNA was synthesized using Superscript III reverse transcriptase (Life Technologies). Then PCR was carried out using the synthesized cDNA as templates and gene-specific primers (see Supplemental Table 2). The primers were designed based on different exons to span the intervening intron and avoid amplification of contaminating genomic DNA.

2.7. Western blotting

Cells were incubated on ice with RIPA buffer containing protease inhibitors (Complete Mini, EDTA-free; Roche, Basel, Switzerland) and a phosphatase inhibitor cocktail (NacalaiTesque). The cell lysates were then resolved by SDS-polyacrylamide gel electrophoresis, followed by immunoblotting. The primary antibodies used are shown in Supplementary Table 3. The signals were detected using a LAS3000 (Fujifilm, Japan). Band intensities were measured by ImageJ software (NIH).

2.8. Statistical analysis

Unless otherwise noted, inter-group differences were analyzed using analysis of variance (ANOVA) followed by the Tukey's post-hoc test with GraphPad Prism 5 (GraphPad Software, CA, USA).

3. Results

3.1. bFGF promotes self-renewal of CM ESCs on feeder cells

bFGF and LIF have been reported to be essential for the maintenance of human and mouse ESCs, respectively [3,12–14,23–27], and either or both of these growth factors were considered to be required for the maintenance of CM ESCs. To determine the optimal condition for culturing CM ESCs, we first examined the expression of receptors for bFGF (FGFR1, FGFR2, FGFR3, and FGFR4) and LIF (LIFR and gp130). RT-PCR analysis demonstrated that all of these receptors were expressed in the CM ESCs (Fig. 1A), suggesting that both growth factors play important roles in the biology of CM ESCs.

In culture, ESCs are generally known to spontaneously differentiate. However, the addition of appropriate growth factors inhibits such spontaneous differentiation. To evaluate the effects of bFGF and LIF on the proliferation and differentiation of CM ESCs in vitro, we passaged CM ESCs at a ratio of 1:3 every three days for three passages, and then counted the numbers of undifferentiated OCT3/4$^+$ cells. We found that the proportion of OCT3/4$^+$ cells was unchanged regardless of the addition of bFGF or LIF (Fig. 1B). However, the numbers of OCT3/4$^+$ cells were significantly increased by the addition of bFGF, but not LIF, compared with those of controls cultured without bFGF and LIF (Fig. 1C). Similar results were obtained when the cells were cultured for more than ten passages (Supplementary Fig. S1 and data not shown). The above experiments were performed using CM40 cell line, and similar results were obtained with Cj11 cell line (Supplementary Fig. S2). These results strongly suggest that bFGF promotes the proliferation of CM ESCs rather than maintaining the undifferentiated state of CM ESCs.

3.2. bFGF-PI3K-AKT pathway supports self-renewal of CM ESCs on feeder cells

bFGF and its downstream PI3K-AKT and MEK-ERK pathways are important for the self-renewal of human ESCs [2,3,5,6]. We therefore examined whether these pathways were activated by bFGF for CM ESC self-renewal on feeder cells. CM ESCs were cultured overnight in medium lacking knockout serum replacement (KSR) and any growth factors. Then, we added bFGF (5 ng/ml), and examined the activation of AKT and ERK1/2 in the cells by Western blotting.

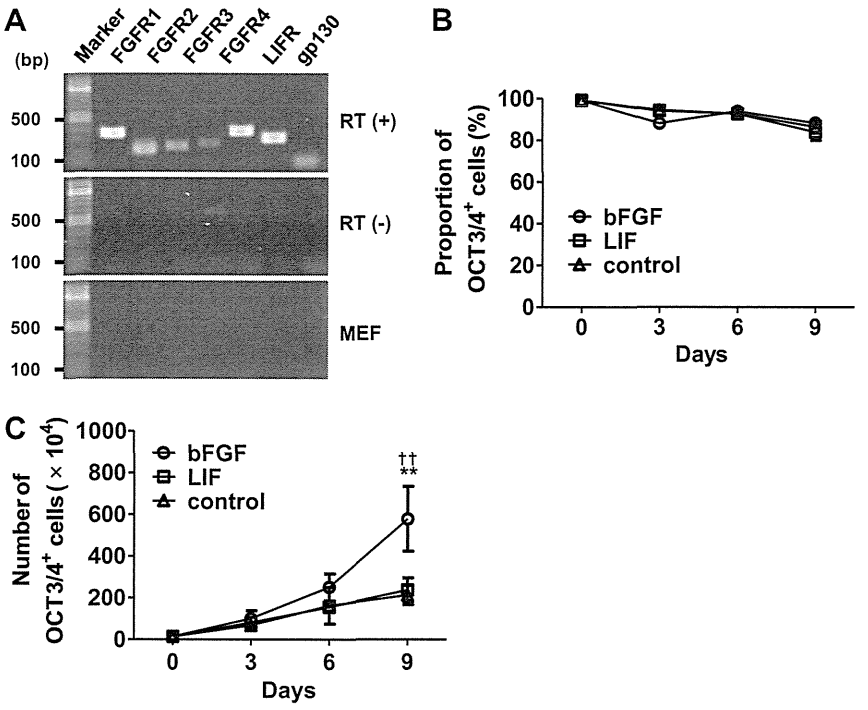

Fig. 1. bFGF promotes self-renewal of CM ESCs in the presence of feeder support. (A) RT-PCR analysis showing the expression of FGFR1, FGFR2, FGFR3, FGFR4, LIFR, and gp130 genes in CM ESCs (CM40). (B) No effect of bFGF on the proportion of OCT3/4$^+$ cells. CM ESCs (CM40; 1.4×10^5) were seeded on mitomycin C (MMC)-treated MEFs and cultured with LIF (open square), bFGF (open circle), or without growth factors (control; open triangle). The percentage of OCT3/4$^+$ cells was determined by FCM. (C) Enhancement of undifferentiated CM ESC growth by bFGF. CM ESCs (CM40; 1.4×10^5) were seeded on mitomycin C (MMC)-treated MEFs and cultured with LIF (open square), bFGF (open circle), or without growth factors (control; open triangle). The number of cells was then counted by trypan blue exclusion. The number of OCT3/4$^+$ cells was determined by multiplying the number of cells by the percentage of OCT3/4$^+$ cells and the passage ratio together. Data are shown as the mean ± SD ($n = 4$). $^{**}P < 0.01$ (bFGF vs. control) and $^{\dagger\dagger}P < 0.01$ (bFGF vs. LIF). Note that all of PCR in (A) was performed with 30 cycles, and no bands were detected for FGFR expression in MEFs in (A), however, they were faintly done when PCR was performed with 40 cycles.

The results showed that the band intensity of phosphorylated AKT was significantly increased after the treatment with bFGF, while that of phosphorylated ERK1/2 was not changed (Fig. 2A and B). These data suggested that PI3K-AKT, but not MEK-ERK, pathway was activated by bFGF in CM ESCs under feeder-dependent culture condition.

Next, to examine whether bFGF-PI3K-AKT pathway plays any roles in the maintenance of self-renewal of CM ESCs, the cells were cultured in medium containing bFGF in the presence or absence of the PI3K inhibitor, LY294002. We found that the proportion of OCT3/4$^+$ cells was maintained at approximately 90% for at least three passages when the cells were cultured without LY294002, whereas it was gradually decreased when the cells were cultured with LY294002 (day0, 96.75 ± 2.83% vs. day9, 57.97 ± 16.76%, Fig. 2C). In addition, OCT3/4$^+$ cell proliferation was inhibited in the presence of LY294002 (day9, bFGF, $7.61 \pm 1.59 \times 10^6$ cells vs. bFGF+LY294002, $2.36 \pm 1.25 \times 10^6$ cells, Fig. 2D). Additionally, even when bFGF was not added, the proportion of OCT3/4$^+$ cells was significantly reduced by the treatment with LY294002 (Fig. 2C), indicating that PI3K-AKT pathway is activated by unknown factors from MEFs and play roles for self-renewal of CM ESCs. Overall, these results strongly suggest that bFGF-PI3K-AKT pathway is essential for the self-renewal of CM ESCs under feeder-dependent culture condition.

To examine the expression of OCT3/4, we used an antibody against amino acids 1–134 of human OCT3/4 (monoclonal OCT3/4 antibody, sc-5279) that was known to be useful for detecting the expression of CM OCT3/4 [28]. And recent study reported that another antibody raised against amino acids 1–19 of human OCT3/4 (polyclonal OCT3/4 antibody, sc-8628) was more useful to detect ESC-specific OCT3/4 [29]. Thus we performed immunocytochemistry and FCM analysis using sc-8628, and obtained the similar results (Supplementary Fig. S3).

3.3. bFGF and TGFβ signaling cooperate to maintain the undifferentiated state of CM ESCs under feeder-free conditions

All of the experiments described above were performed with feeder support. Thus, the various secreted factors including cytokines and adhesion molecules might have affected the results. To examine the dependency of CM ESCs on feeder cells, CM ESCs were cultured on a high or low density of feeder cells, and then the undifferentiated state was examined by immunocytochemistry using an anti-NANOG antibody (Supplementary Fig. S1). We found that CM ESCs on low-density feeder cells lost their expression of NANOG after four passages, whereas those on high-density feeder cells maintained NANOG expression even after ten passages (Supplementary Fig. S1). Therefore, it is conceivable that the self-renewal of CM ESCs is maintained by unknown factors derived from feeder cells.

Chen et al. showed that Essential 8 medium (Dulbecco's modified Eagle's medium/F12 supplemented with L-ascorbic acid-2-phosphate magnesium, insulin, transferrin, sodium selenium, $NaHCO_3$, bFGF, and TGFβ) supports the self-renewal of human ESCs and iPSCs under feeder-free conditions [30]. To clarify the essential growth factors required for maintaining the undifferentiated state of CM ESCs, CM ESCs were cultured under feeder-free condition. We found that CM ESCs could be cultured on Matrigel in Essential 8 medium without feeder support, although they could not be maintained for more than three passages (data not shown). Next, we cultured CM ESCs on Matrigel in Essential 6 medium lacking bFGF and TGFβ overnight, and then the activation of signaling

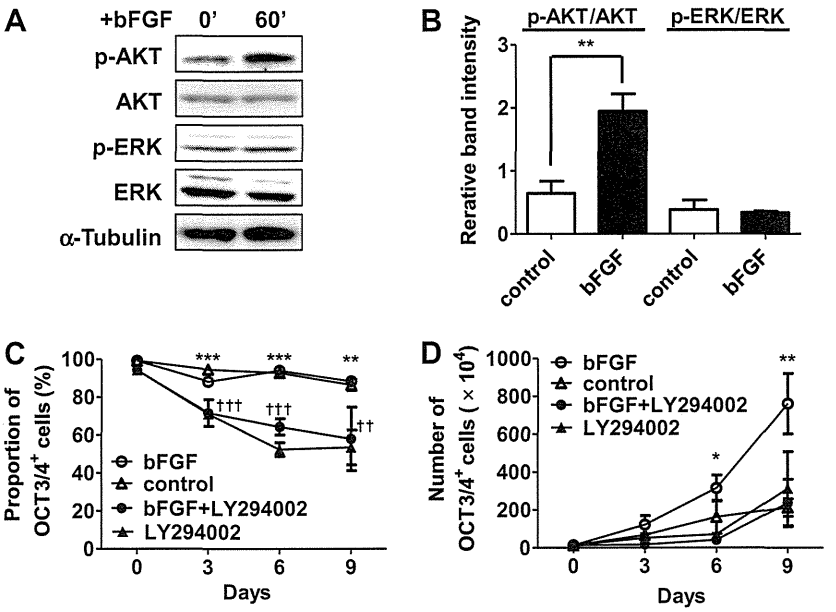

Fig. 2. bFGF-PI3K-AKT pathway supports self-renewal of CM ESCs. (A) Western blot analysis showing the activation of AKT by bFGF in CM ESCs. CM40 cells were starved of bFGF and KSR overnight, and then stimulated with 5 ng/ml of bFGF for the indicated durations. AKT, ERK1/2 and α-Tubulin are shown as loading controls. The relative band intensities of p-AKT/AKT and p-ERK/ERK are shown in (B). Band intensities were measured by ImageJ software. Data are shown as the mean ± SD. The Student's *t*-test was used to test inter-group differences. $^{**}P < 0.01$. (C) Inhibition of self-renewal by LY294002. CM ESCs (CM40; 1.4×10^5) were seeded on MMC-treated MEFs and cultured in medium containing bFGF (open circle), control medium (open triangle), bFGF+LY294002 (closed circle) or LY294002 (closed triangle). The percentage of OCT3/4$^+$ cells was then determined by FCM at the indicated day as shown in (C). The number of live cells was counted by trypan blue exclusion. Growth curves were generated by multiplying the number of live cells by the percentage of OCT3/4$^+$ cells and passage ratio together as shown in (D). Data are shown as the mean ± SD. bFGF, $n = 4$; control, $n = 4$; bFGF+LY294002, $n = 3$; LY294002, $n = 3$; $^{*}P < 0.05$, $^{**}P < 0.01$, and $^{***}P < 0.005$, bFGF vs. control; $^{\dagger\dagger}P < 0.01$ and $^{\dagger\dagger\dagger}P < 0.005$, bFGF+LY294002 or LY294002 vs. control.

pathways known to maintain mouse and human ESCs (bFGF-PI3K-AKT, bFGF-MEK-ERK, TGFβ-SMAD2/3, and LIF-JAK-STAT3 pathways) were analyzed by Western blotting after the addition of bFGF, TGFβ, or LIF to the medium. We found that phosphorylation of AKT and ERK was increased by the addition of bFGF, while it was decreased by the treatment with LY294002 or PD0325901, suggesting that both of AKT and ERK were activated downstream of bFGF under feeder-free condition (Fig. 3A and B). And the addition of TGFβ resulted in an increase of phosphorylated SMAD2/3 (Fig. 3A and B), suggesting that SMAD2/3 was activated downstream of TGFβ. Moreover, the addition of LIF resulted in an increase of phosphorylated STAT3, suggesting that STAT3 was activated downstream of LIF (Supplementary Figs. S4B and D). These results suggested that bFGF-PI3K-AKT, bFGF-MEK-ERK, TGFβ-SMAD2/3 and LIF-JAK-STAT3 pathways known to regulate self-renewal of human or mouse ESCs were activated in CM ESCs under feeder-free condition. It should be noted that ERK was not activated by 5 ng/ml of bFGF that was used for the culture on feeder cells as described in Fig. 2A and B (Supplementary Fig. S4B), but it was remarkably activated by 100 ng/ml of bFGF generally used for feeder-free culture of human ESCs (Fig. 3A and B) [30].

Next, to determine the growth factors maintaining the undifferentiated state of CM ESCs under feeder-free condition, CM ESCs were cultured in the feeder-free system with various combinations of growth factors, followed by analysis of their undifferentiated state morphologically and immunocytochemically. Most of the colonies cultured in Essential 6 medium with bFGF, bFGF+TGFβ, bFGF+LIF, or bFGF+TGFβ+LIF showed a well-packed appearance, and a majority of the cells expressed NANOG (Fig. 3C). In contrast, most of the colonies cultured in Essential 6 medium with TGFβ, LIF, or TGFβ+LIF showed an unpacked appearance, and a majority of the cells did not express NANOG (Fig. 3C). Moreover, NANOG$^+$ and well-packed colonies were found at the highest proportion (98.00 ± 0.88%) when the cells were cultured in the presence of TGFβ+bFGF (Fig. 3D). In addition, almost all of the colonies were positive for OCT3/4, SOX2, SSEA-4, TRA1-60 and TRA1-81 (Supplementary Fig. S3), and these colony forming cells kept the capability of differentiating three lineages (Supplementary Fig. S5). This observation indicates that the addition of both TGFβ and bFGF is the most appropriate growth factor combination for maintenance of the undifferentiated state of CM ESCs under feeder-free condition, which is similar to a characteristic of human ESCs [2,6,9–11].

3.4. CM ESCs show phenotypes similar to those of human ESCs and mouse EpiSCs

Human ESCs and mouse EpiSCs share a number of similar phenotypes as shown in Table 1 [7,8]. CM ESCs formed flattened colonies and expressed NANOG as well as markers for both mouse EpiSCs and human ESCs, such as T, CER1, EOMES, FOXA2, GATA6, and SOX17 (Supplementary Figs. S1 and S6A) [7]. Moreover, bFGF and TGFβ signalings play crucial roles in maintaining the undifferentiated state of human ESCs and mouse EpiSCs [2,7,8,11,30], and the same roles of these signaling pathways were also found in CM ESCs (Fig. 3C and D).

Previous reports have shown that apoptosis of human ESCs and mouse EpiSCs is induced by culturing after complete dissociation [31,32]. Watanabe et al. showed that dissociation-induced apoptosis of human ESCs is suppressed by treatment with the Rho-associated kinase (ROCK) inhibitor Y27632 [33]. To examine whether dissociation-induced apoptosis of human ESCs and mouse EpiSCs was similarly found in CM ESCs, colonies of CM ESCs were dissociated into single cells by trypsinization, and then the cells were plated on Matrigel-coated dishes with or without Y27632. Compared with untreated controls, we found that Y27632-treated CM ESCs produced

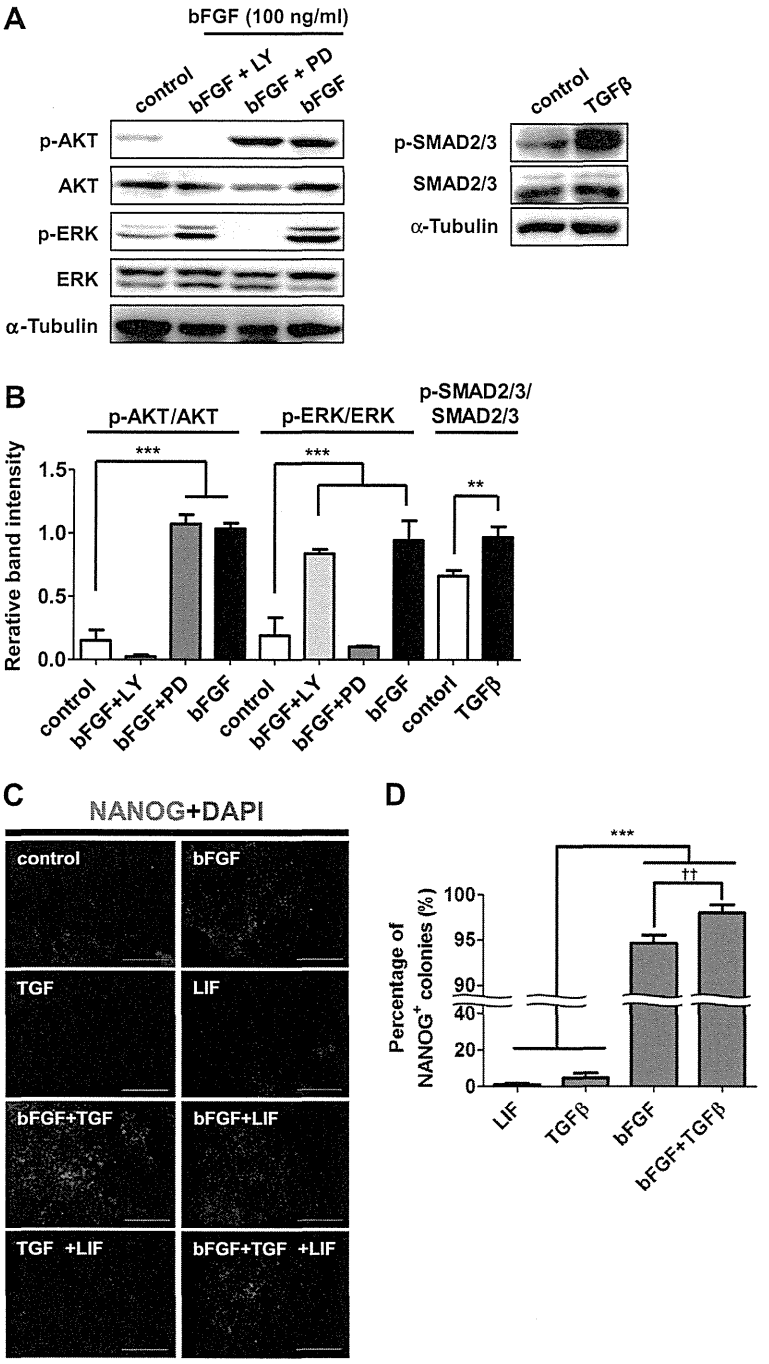

Fig. 3. bFGF and TGFβ maintain the undifferentiated state of CM ESCs under feeder-free conditions. (A) Western blot showing the activation of AKT, ERK1/2 and SMAD2/3 by 100 ng/ml of bFGF or 2 ng/ml of TGFβ for 30 min in CM ESCs. CM40 were starved of growth factors overnight and then pre-treated with LY294002 or PD0325901for 1 h before stimulation with bFGF. AKT, ERK1/2, SMAD2/3, and α-Tubulin are shown as loading controls. The relative band intensities of p-AKT/AKT, p-ERK/ERK and p-SMAD2/3/SMAD2/3 are shown in (B). Band intensities were measured by ImageJ software. Data are shown as the mean±SD. One-way ANOVA followed by the Tukey's post-hoc test was used to test inter-group differences. $^{**}P < 0.01$ and $^{***}P < 0.005$. (C) Immunocytochemical analyses of NANOG expression in CM ESCs (CM40) cultured with various growth factors for 4 days. Merged images of NANOG (red) and nuclei (DAPI; blue) are shown. Scale bars represent 200 μm. NANOG expression in cells cultured without any growth factors is shown as a control. (D) Proportion of NANOG$^+$ colonies. The percentage of NANOG$^+$ colonies cultured with various growth factors was analyzed by immunocytochemistry. For statistical analyses, 300 colonies were examined in each experiment ($n = 3$). Data are shown as the mean ± SD. One-way ANOVA followed by the Tukey's post-hoc test was used to test inter-group differences. $^{***}P < 0.005$. The difference between bFGF- and bFGF+TGFβ-treated cells was statistically analyzed using the Student's *t*-test. $^{††}P < 0.01$.

significantly more colonies, suggesting that dissociation-induced apoptosis of CM ESCs occurred and was suppressed by Y27632 (Supplementary Figs. S6B and S6C). Thus, we concluded that CM ESCs are similar to human ESCs and mouse EpiSCs.

4. Discussion

Recent advances in the field of basic research for pluripotent stem cells such as the generation of ESCs, iPSCs and stimulus-trig-

Table 1
The characters of mouse EpiSCs and mouse, human and CM ESCs.

Morphology of colony		Mouse ESCs Small, dome	Mouse EpiSCs Large, flat	Human ESCs Large, flat	CM ESCs Large, flat
Growth factor dependency	LIF	+	–	–	–
	bFGF	–	+	+	+
	TGFβ/activin	–	+	+	+
Marker expression	NANOG	+	+	+	+
	OCT3/4	+	+	+	+
	T (brachyury)	–	+	+	+
	CER1	–	+	+	+
	EOMES	–	+	+	+
	FOXA2	–	+	+	+
	GATA6	–	+	+	+
	SOX17	–	+	+	+
Tolerance to single cell dissociation		+	–	–	–
Contribution in chimera		+	–	N/D	N/D

N/D = not determined.

gered acquisition of pluripotency (STAP) cells have given us realistic expectations for human regenerative medicine [22,34–38]. And the need for the development of methods to test new therapeutic approach using such cells is increasing. CM is a useful experimental animal that can suit such needs, and therefore, the characterization of CM ESCs is important. In this study, we investigated essential signaling pathways for the self-renewal of CM ESCs under feeder-dependent and feeder-free culture conditions.

LIF has been widely used to establish and maintain non-human primate ESCs [15,17,18,39–42], although some researchers claim that LIF cannot maintain the self-renewal capacity of these cells [16,41–43]. We found that LIF did not affect the capacity for self-renewal of CM ESCs (Figs. 1 and 3), although it activated the JAK-STAT3 pathway (Supplementary Fig. S3). More extensive studies are needed to further explore the roles of the LIF-JAK-STAT3 pathway in CM ESCs. In our previous report, the expression of LIFR was not found in undifferentiated CM ESCs [15], but it was found in this study after repetitive experiments (Fig. 1A). This discrepancy was considered to be caused by the detection threshold of RT-PCR under different conditions, particularly PCR primers used in our previous report were human LIFR sequence-originated because there were no available marmoset genomic sequence data.

We also found that the self-renewal of CM ESCs cultured on feeder cells was remarkably promoted by bFGF, which is similar to the characteristic of human ESCs (Fig. 1). However, even in the absence of bFGF, most CM ESCs could be maintained in an undifferentiated state by culture on feeder cells, although they showed slower growth compared to those cultured in bFGF containing medium (Fig. 1B and C). This observation indicates that growth factors secreted from feeder cells such as activin, noggin and bFGF, maintain the undifferentiated state of CM ESCs [44,45]. Indeed, CM ESC colonies cultured on low-density feeder cells differentiated within four passages (Supplementary Fig. S1).

Previous studies have demonstrated the critical roles of PI3K-AKT and MEK-ERK pathways in the self-renewal of human ESCs [2–6]. Our results showed that AKT, but not ERK1/2, was activated by the addition of bFGF (5 ng/ml), while ERK1/2 was continuously activated even in the absence of bFGF on feeder support (Fig. 2A). Moreover, inhibition of either MEK-ERK or PI3K-AKT pathways resulted in reduced self-renewal of CM ESCs (Fig. 2 and Supplementary Fig. S7). Therefore, activation of the PI3K-AKT pathway downstream of bFGF as well as the MEK-ERK pathway by unknown mechanisms is required for self-renewal of CM ESCs on feeder support. On the other hand, both AKT and ERK1/2 were activated by the addition of bFGF (100 ng/ml) under feeder-free condition (Fig. 3A and B). And treatment with LY294002 resulted in the elevated expression of endoderm and mesoderm markers, and treatment with PD0325901 caused the reduced expression of these markers, indicating that modulation of these pathways affects the differentiation process in CM ESCs (Supplementary Fig. S8). We are now extensively investigating the effect of these inhibitors on the differentiation process of CM ESCs induced by the treatment with specific cytokines and EB formation assay.

Several studies have demonstrated differences in the mechanisms of ESC self-renewal between mice and humans. Mouse ESCs require LIF for their self-renewal, whereas human ESCs require bFGF and TGFβ. Mouse EpiSCs originating from post-implantation embryos depend on bFGF and TGFβ, and show characteristics similar to those of human ESCs originating from the inner cells mass of blastocysts as shown in Table 1 [7,8,10]. Mouse EpiSCs are therefore considered to be the counterpart of human ESCs. In this study, we demonstrated that CM ESCs were very similar to human ESCs and mouse EpiSCs in terms of their morphology, gene expression, growth factor dependency for self-renewal, and vulnerability to single cell dissociation.

Our findings strongly suggest that CM ESCs are phenotypically similar to human ESCs. Therefore, CM ESCs may facilitate the development of valuable preclinical experimental systems to test new therapeutic modalities for incurable human diseases, particularly in the field of regenerative medicine.

Acknowledgments

We thank Michiko Ushijima for administrative assistance, Yoko Nagai and the members of Tani laboratory for their constructive criticisms and technical support. This work was supported by a grant from the Project for Realization of Regenerative Medicine (K. Tani, 08008010) and KAKENHI (T. Marumoto, 23590465) from the Ministry of Education, Culture, Sports, Science and Technology (MEXT), Japan.

Appendix A. Supplementary data

Supplementary data associated with this article can be found, in the online version, at http://dx.doi.org/10.1016/j.fob.2014.02.007.

References

[1] Hibino, H. et al. (1999) The common marmoset as a target preclinical primate model for cytokine and gene therapy studies. Blood 93, 2839–2848.
[2] Singh, A.M. et al. (2012) Signaling network crosstalk in human pluripotent cells: a Smad2/3-regulated switch that controls the balance between self-renewal and differentiation. Cell Stem Cell 10, 312–326.
[3] Armstrong, L. et al. (2006) The role of PI3K/AKT, MAPK/ERK and NFκβ signalling in the maintenance of human embryonic stem cell pluripotency and

viability highlighted by transcriptional profiling and functional analysis. Hum. Mol. Genet. 15, 1894–1913.
[4] Li, J. et al. (2007) MEK/ERK signaling contributes to the maintenance of human embryonic stem cell self-renewal. Differentiation 75, 299–307.
[5] Na, J., Furue, M.K. and Andrews, P.W. (2010) Inhibition of ERK1/2 prevents neural and mesendodermal differentiation and promotes human embryonic stem cell self-renewal. Stem Cell Res. 5, 157–169.
[6] McLean, A.B. et al. (2007) Activin a efficiently specifies definitive endoderm from human embryonic stem cells only when phosphatidylinositol 3-kinase signaling is suppressed. Stem Cells 25, 29–38.
[7] Tesar, P.J., Chenoweth, J.G., Brook, F.A., Davies, T.J., Evans, E.P., Mack, D.L., Gardner, R.L. and McKay, R.D.G. (2007) New cell lines from mouse epiblast share defining features with human embryonic stem cells. Nature 448, 196–199.
[8] Brons, I.G.M. et al. (2007) Derivation of pluripotent epiblast stem cells from mammalian embryos. Nature 448, 191–195.
[9] James, D., Levine, A.J., Besser, D. and Hemmati-Brivanlou, A. (2005) TGFβ/activin/nodal signaling is necessary for the maintenance of pluripotency in human embryonic stem cells. Development 132, 1273–1282.
[10] Greber, B. et al. (2010) Conserved and divergent roles of FGF signaling in mouse epiblast stem cells and human embryonic stem cells. Cell Stem Cell 6, 215–226.
[11] Vallier, L., Alexander, M. and Pedersen, R.A. (2005) Activin/Nodal and FGF pathways cooperate to maintain pluripotency of human embryonic stem cells. J. Cell Sci. 118, 4495–4509.
[12] Williams, R.L. et al. (1988) Myeloid leukaemia inhibitory factor maintains the developmental potential of embryonic stem cells. Nature 336, 684–687.
[13] Niwa, H., Burdon, T., Chambers, I. and Smith, A. (1998) Self-renewal of pluripotent embryonic stem cells is mediated via activation of STAT3. Genes Dev. 12, 2048–2060.
[14] Takahashi, K., Murakami, M. and Yamanaka, S. (2005) Role of the phosphoinositide 3-kinase pathway in mouse embryonic stem (ES) cells. Biochem. Soc. Trans. 33, 1522.
[15] Sasaki, E. et al. (2005) Establishment of novel embryonic stem cell lines derived from the common marmoset (Callithrix jacchus). Stem Cells 23, 1304–1313.
[16] Thomson, J.A., Kalishman, J., Golos, T.G., Durning, M., Harris, C.P. and Hearn, J.P. (1996) Pluripotent cell lines derived from common marmoset (Callithrix jacchus) blastocysts. Biol. Reprod. 55, 254–259.
[17] Müller, T., Fleischmann, G., Eildermann, K., Mätz-Rensing, K., Horn, P.A., Sasaki, E. and Behr, R. (2009) A novel embryonic stem cell line derived from the common marmoset monkey (Callithrix jacchus) exhibiting germ cell-like characteristics. Hum. Reprod. 24, 1359–1372.
[18] Shimada, H. et al. (2012) Efficient derivation of multipotent neural stem/progenitor cells from non-human primate embryonic stem cells. PLoS One 7, e49469.
[19] Maeda, T., Kurita, R., Yokoo, T., Tani, K. and Makino, N. (2011) Telomerase inhibition promotes an initial step of cell differentiation of primate embryonic stem cell. Biochem. Biophys. Res. Commun. 407, 491–494.
[20] Shimoji, K. et al. (2010) G-CSF promotes the proliferation of developing cardiomyocytes in vivo and in derivation from ESCs and iPSCs. Cell Stem Cell 6, 227–237.
[21] Chen, H. et al. (2008) Common marmoset embryonic stem cell can differentiate into cardiomyocytes. Biochem. Biophys. Res. Commun. 369, 801–806.
[22] Takahashi, K., Tanabe, K., Ohnuki, M., Narita, M., Ichisaka, T., Tomoda, K. and Yamanaka, S. (2007) Induction of pluripotent stem cells from adult human fibroblasts by defined factors. Cell 131, 861–872.
[23] Niwa, H., Ogawa, K., Shimosato, D. and Adachi, K. (2009) A parallel circuit of LIF signalling pathways maintains pluripotency of mouse ES cells. Nature 460, 118–122.
[24] Levenstein, M.E., Ludwig, T.E., Xu, R.H., Llanas, R.A., VanDenHeuvel-Kramer, K., Manning, D. and Thomson, J.A. (2006) Basic fibroblast growth factor support of human embryonic stem cell self-renewal. Stem Cells 24, 568–574.
[25] Xu, R.H., Peck, R.M., Li, D.S., Feng, X., Ludwig, T. and Thomson, J.A. (2005) Basic FGF and suppression of BMP signaling sustain undifferentiated proliferation of human ES cells. Nat. Methods 2, 185–190.
[26] Xu, C. et al. (2005) Basic fibroblast growth factor supports undifferentiated human embryonic stem cell growth without conditioned medium. Stem Cells 23, 315–323.
[27] Dahéron, L., Opitz, S.L., Zaehres, H., Lensch, W.M., Andrews, P.W., Itskovitz-Eldor, J. and Daley, G.Q. (2004) LIF/STAT3 signaling fails to maintain self-renewal of human embryonic stem cells. Stem Cells 22, 770–778.
[28] Wu, Y., Zhang, Y., Mishra, A., Tardif, S.D. and Hornsby, P.J. (2010) Generation of induced pluripotent stem cells from newborn marmoset skin fibroblasts. Stem Cell Res. 4, 180–188.
[29] Warthemann, R., Eildermann, K., Debowski, K. and Behr, R. (2012) False-positive antibody signals for the pluripotency factor OCT4A (POU5F1) in testis-derived cells may lead to erroneous data and misinterpretations. Mol. Hum. Reprod. 18, 605–612.
[30] Chen, G. et al. (2011) Chemically defined conditions for human iPSC derivation and culture. Nat. Methods 8, 424–429.
[31] Amit, M., Carpenter, M.K., Inokuma, M.S., Chiu, C.-P., Harris, C.P., Waknitz, M.A., Itskovitz-Eldor, J. and Thomson, J.A. (2000) Clonally derived human embryonic stem cell lines maintain pluripotency and proliferative potential for prolonged periods of culture. Dev. Biol. 227, 271–278.
[32] Ohgushi, M. et al. (2010) Molecular pathway and cell state responsible for dissociation-induced apoptosis in human pluripotent stem cells. Cell Stem Cell 7, 225–239.
[33] Watanabe, K. et al. (2007) A ROCK inhibitor permits survival of dissociated human embryonic stem cells. Nat. Biotechnol. 25, 681–686.
[34] Takahashi, K. and Yamanaka, S. (2006) Induction of pluripotent stem cells from mouse embryonic and adult fibroblast cultures by defined factors. Cell 126, 663–676.
[35] Thomson, J.A., Itskovitz-Eldor, J., Shapiro, S.S., Waknitz, M.A., Swiergiel, J.J., Marshall, V.S. and Jones, J.M. (1998) Embryonic stem cell lines derived from human blastocysts. Science 282, 1145–1147.
[36] Evans, M.J. and Kaufman, M.H. (1981) Establishment in culture of pluripotential cells from mouse embryos. Nature 292, 154–156.
[37] Obokata, H., Wakayama, T., Sasai, Y., Kojima, K., Vacanti, M.P., Niwa, H., Yamato, M. and Vacanti, C.A. (2014) Stimulus-triggered fate conversion of somatic cells into pluripotency. Nature 505, 641–647.
[38] Obokata, H. et al. (2014) Bidirectional developmental potential in reprogrammed cells with acquired pluripotency. Nature 505, 676–680.
[39] Shimozawa, N., Nakamura, S., Takahashi, I., Hatori, M. and Sankai, T. (2010) Characterization of a novel embryonic stem cell line from an ICSI-derived blastocyst in the African green monkey. Reproduction 139, 565–573.
[40] Simerly, C.R. et al. (2009) Establishment and characterization of baboon embryonic stem cell lines: An Old World Primate model for regeneration and transplantation research. Stem Cell Res. 2, 178–187.
[41] Suemori, H. et al. (2001) Establishment of embryonic stem cell lines from cynomolgus monkey blastocysts produced by IVF or ICSI. Dev. Dyn. 222, 273–279.
[42] Thomson, J.A., Kalishman, J., Golos, T.G., Durning, M., Harris, C.P., Becker, R.A. and Hearn, J.P. (1995) Isolation of a primate embryonic stem cell line. Proc. Nat. Acad. Sci. 92, 7844–7848.
[43] Mitalipov, S., Kuo, H.C., Byrne, J., Clepper, L., Meisner, L., Johnson, J., Zeier, R. and Wolf, D. (2006) Isolation and characterization of novel rhesus monkey embryonic stem cell lines. Stem Cells 24, 2177–2186.
[44] Wang, G. et al. (2005) Noggin and bFGF cooperate to maintain the pluripotency of human embryonic stem cells in the absence of feeder layers. Biochem. Biophys. Res. Commun. 330, 934–942.
[45] Beattie, G.M., Lopez, A.D., Bucay, N., Hinton, A., Firpo, M.T., King, C.C. and Hayek, A. (2005) Activin A maintains pluripotency of human embryonic stem cells in the absence of feeder layers. Stem Cells 23, 489–495.

Research Article

Cancer Immunology Research

TLR7 Ligand Augments GM-CSF–Initiated Antitumor Immunity through Activation of Plasmacytoid Dendritic Cells

Megumi Narusawa[1], Hiroyuki Inoue[1,2,3], Chika Sakamoto[1], Yumiko Matsumura[1], Atsushi Takahashi[1], Tomoko Inoue[1], Ayumi Watanabe[1], Shohei Miyamoto[1], Yoshie Miura[1], Yasuki Hijikata[3], Yoshihiro Tanaka[3], Makoto Inoue[5], Koichi Takayama[2], Toshihiko Okazaki[4], Mamoru Hasegawa[5], Yoichi Nakanishi[2], and Kenzaburo Tani[1,3]

Abstract

Vaccination with irradiated granulocyte macrophage colony-stimulating factor (GM-CSF)–transduced autologous tumor cells (GVAX) has been shown to induce therapeutic antitumor immunity. However, its effectiveness is limited. We therefore attempted to improve the antitumor effect by identifying little-known key pathways in GM-CSF–sensitized dendritic cells (GM-DC) in tumor-draining lymph nodes (TDLN). We initially confirmed that syngeneic mice subcutaneously injected with poorly immunogenic Lewis lung carcinoma (LLC) cells transduced with Sendai virus encoding GM-CSF (LLC/SeV/GM) remarkably rejected the tumor growth. Using cDNA microarrays, we found that expression levels of type I interferon (IFN)–related genes, predominantly expressed in plasmacytoid DCs (pDC), were significantly upregulated in TDLN-derived GM-DCs and focused on pDCs. Indeed, mouse experiments demonstrated that the effective induction of GM-CSF–induced antitumor immunity observed in immunocompetent mice treated with LLC/SeV/GM cells was significantly attenuated when pDC-depleted or IFNα receptor knockout ($IFNAR^{-/-}$) mice were used. Importantly, in both LLC and CT26 colon cancer–bearing mice, the combinational use of imiquimod with autologous GVAX therapy overcame the refractoriness to GVAX monotherapy accompanied by tolerability. Mechanistically, mice treated with the combined vaccination displayed increased expression levels of CD86, CD9, and Siglec-H, which correlate with an antitumor phenotype, in pDCs, but decreased the ratio of $CD4^+CD25^+FoxP3^+$ regulatory T cells in TDLNs. Collectively, these findings indicate that the additional use of imiquimod to activate pDCs with type I IFN production, as a positive regulator of T-cell priming, could enhance the immunologic antitumor effects of GVAX therapy, shedding promising light on the understanding and treatment of GM-CSF–based cancer immunotherapy. *Cancer Immunol Res; 2(6); 568–80. ©2014 AACR.*

Introduction

In recent clinical trials of patients with diverse solid cancers, cancer immunotherapy such as therapeutic vaccination with granulocyte macrophage colony-stimulating factor (GM-CSF) gene-transduced tumor vaccines (GVAX), as well as sipuleucel-T (Provenge; Dendreon), the first FDA-approved GM-CSF–based therapeutic dendritic cell (DC) vaccine for prostate cancer, induced antitumor immune responses with tolerability (1–3). However, the efficacy of this therapy alone is not satisfactory, raising an urgent need to improve the antitumor effect of GVAX. Although GM-CSF signaling is essential in conventional DC (cDC) maturation, which leads to effective generation of tumor-associated antigen (TAA)-specific T cells and differentiation, the underlying molecular mechanism of how GM-CSF sensitizes and matures DCs (GM-DC, i.e., GM-CSF–sensitized DCs) to trigger host antitumor immunity remains unclear.

Therefore, in this study, we attempted to improve the antitumor effects of GVAX therapy through identification of the key cluster genes upregulated in GM-DCs that operate T-cell priming in tumor-draining lymph nodes (TDLN) by conducting a cDNA microarray analysis. We used a syngeneic Lewis lung carcinoma (LLC)–bearing mouse, which exhibited remarkable tumor regression following subcutaneous administration of fusion (F) gene-deleted nontransmissible Sendai virus vector–mediated GM-CSF gene-transduced LLC (LLC/SeV/GM) cells (4). Using this experimental system, the expression microarray analysis elucidated that pathways involving Toll-like receptor 7 (TLR7) and interferon regulatory factor 7 (IRF7), which induce type I interferon (IFN) production in plasmacytoid DCs (pDC; ref. 5), were upregulated in GM-CSF–activated mature DCs. Further activation of this pathway using

Authors' Affiliations: [1]Department of Molecular Genetics, Medical Institute of Bioregulation; [2]Research Institute for Diseases of the Chest, Graduate School of Medical Sciences; [3]Department of Advanced Cell and Molecular Therapy and [4]Center for Clinical and Translational Research, Kyushu University Hospital, Kyushu University, Fukuoka; and [5]DNAVEC Corporation, Tsukuba, Japan

Note: Supplementary data for this article are available at Cancer Immunology Research Online (http://cancerimmunolres.aacrjournals.org/).

Corresponding Author: Kenzaburo Tani, Department of Molecular Genetics, Medical Institute of Bioregulation, Kyushu University, 3-1-1 Maidashi, Higashi-ku, Fukuoka 812-8582, Japan. Phone: 81-92-642-6449; Fax: 81-92-642-6444; E-mail: taniken@bioreg.kyushu-u.ac.jp

doi: 10.1158/2326-6066.CIR-13-0143

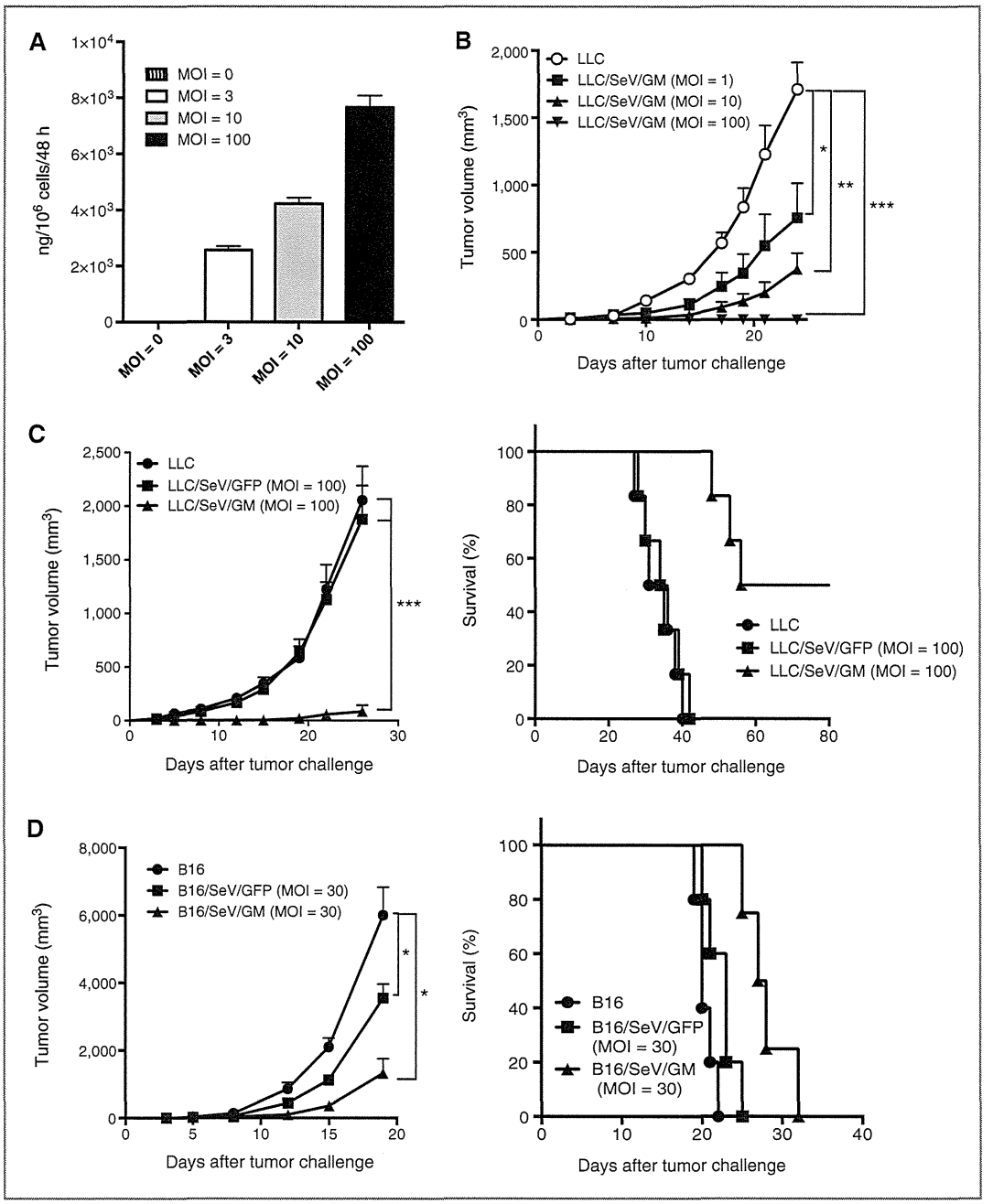

Figure 1. Tumor development of poorly immunogenic LLC and B16F10 cells modified to produce GM-CSF was markedly inhibited. A, dose-escalation studies to assess GM-CSF production from LLC/SeV/GM cells (MOI = 0, 3, 10, and 100). GM-CSF production levels in the supernatants from the 48-hour culture were measured by ELISA. B and C, tumorigenicity assays using LLC cells. B, a total of 3.0×10^5 LLC and LLC/SeV/GM (MOI of 1, 10, or 100) cells were subcutaneously inoculated into the right flank of C57/BL6N mice ($n = 3$). C, a total of 2.0×10^5 LLC, LLC/SeV/GFP, or LLC/SeV/GM (MOI = 100) cells were inoculated into the right flank of C57/BL6N mice ($n = 6$). Significant tumor regression (left) and prolonged survival (right) was shown in mice treated with LLC/SeV/GM cells. D, tumorigenicity assays using B16F10 cells. In total, 1.0×10^5 B16F10, B16/SeV/GFP, or B16/SeV/GM (MOI = 30) cells were inoculated into the right flanks of C57/BL6N mice ($n = 6$). Significant tumor regression (left) and prolonged survival (right) were observed in mice treated with B16/SeV/GM cells. The asterisks indicate statistically significant differences (*, $P < 0.05$; **, $P < 0.01$; ***, $P < 0.001$). Kaplan–Meier survival curves are shown, and mortality was determined by the log-rank test (LLC vs. LLC/SeV/GM and LLC/SeV/GFP vs. LLC/SeV/GM; $P < 0.001$, LLC vs. LLC/SeV/GFP; $P = 0.67$, B16 vs. B16/SeV/GM and B16/SeV/GFP vs. B16/SeV/GM; $P < 0.05$).

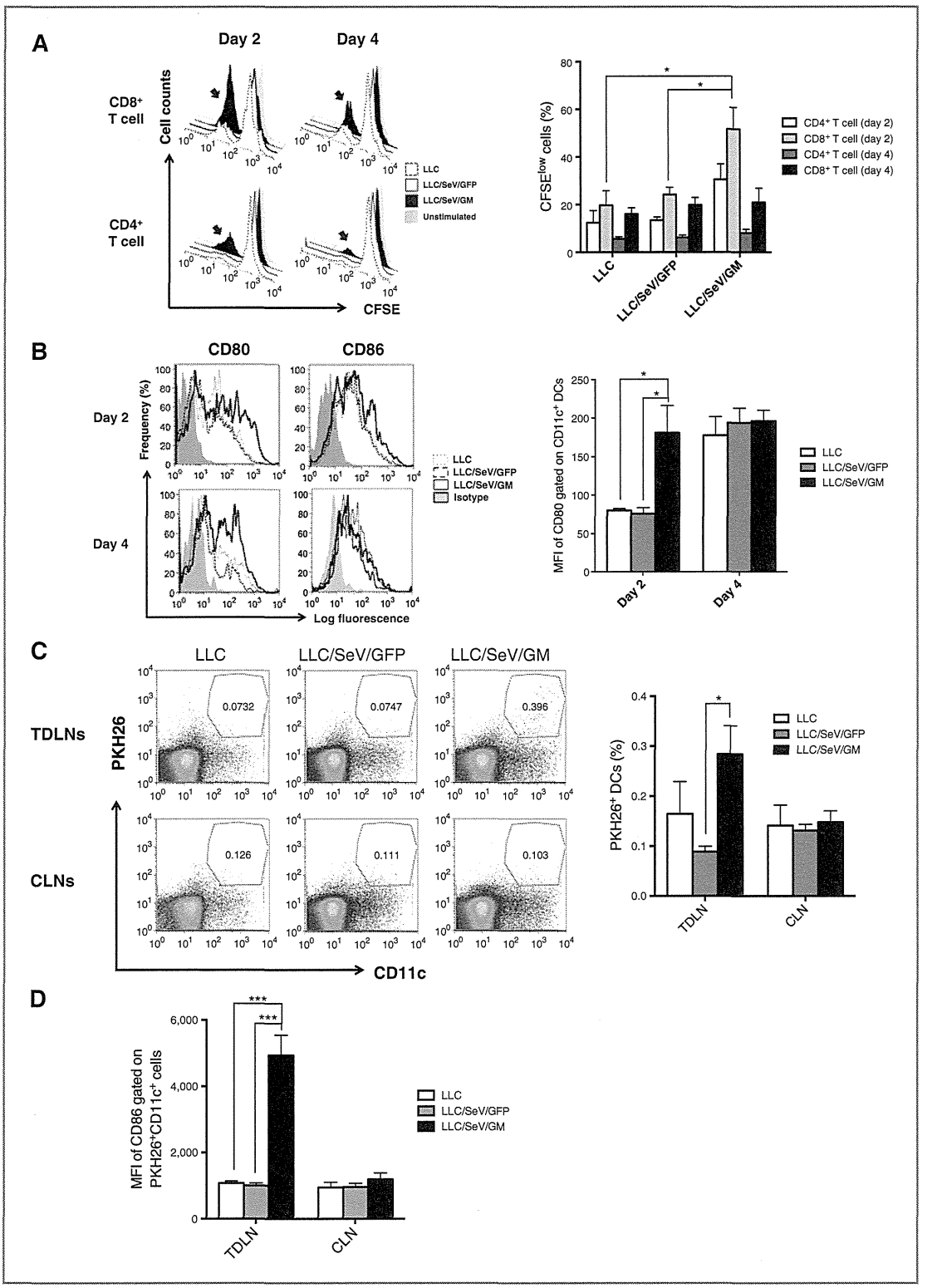
A
Day 2
Day 4
CD8+ T cell
CD4+ T cell
Cell counts
CFSE
LLC
LLC/SeV/GFP
LLC/SeV/GM
Unstimulated
CFSElow cells (%)
CD4+ T cell (day 2)
CD8+ T cell (day 2)
CD4+ T cell (day 4)
CD8+ T cell (day 4)
B
CD80
CD86
Day 2
Day 4
Frequency (%)
Log fluorescence
Isotype
MFI of CD80 gated on CD11c+ DCs
C
LLC
LLC/SeV/GFP
LLC/SeV/GM
TDLNs
CLNs
PKH26
CD11c
0.0732
0.0747
0.396
0.126
0.111
0.103
PKH26+ DCs (%)
TDLN
CLN
D
MFI of CD86 gated on PKH26+CD11c+ cells

Table 1. Canonical pathways identified by IPA

Pathways	−log (*P* value)	Molecules
Role of pattern recognition receptors in recognition of bacteria and viruses	7.42E+00	OAS1, C3, OAS2, IL6, CCL5, Oas1f, OAS3, IFNA1/IFNA13, TLR2, IFIH1, IRF7, DDX58, TLR7, PIK3R6, EIF2AK2
Pathogenesis of multiple sclerosis	5.33E+00	CXCL10, CXCL9, CCL4, CCL5, CXCL11
Activation of IRF by cytosolic pattern recognition receptors	4.38E+00	DHX58, IFIH1, IRF7, DDX58, ZBP1, STAT2, IL6, IFIT2, IFNA1/IFNA13, ISG15
IFN signaling	3.96E+00	IFIT3, IFIT1, OAS1, MX1, IFI35, STAT2, IFNA1/IFNA13
DC maturation	3.01E+00	FCGR2A, HLA-DMB, IL6, MAPK13, FCGR2B, TREM2, IFNA1/IFNA13, FCGR1A, TLR2, COL1A2, IL1RN, FSCN1, PIK3R6, STAT2
Hepatic fibrosis/hepatic stellate cell activation	2.58E+00	COL1A2, CXCL3, FN1, CXCL9, IGF1, PDGFA, CCL21, CD14, MMP13, CCL5, IL6, IFNA1/IFNA13
Role of hypercytokinemia/hyperchemokinemia in the pathogenesis of influenza	2.49E+00	CXCL10, CCL4, IL1RN, CCL5, IL6, IFNA1/IFNA13
Communication between innate and adaptive immune cells	2.47E+00	CXCL10, TLR2, CCL4, IL1RN, TLR7, CCL5, IL6, IFNA1/IFNA13, Ccl9
Role of tissue factor in cancer	2.45E+00	F10, PDIA2, PIK3R6, HCK, MMP13, F7, LIMK2, MAPK13, FGR, F2
LXR/RXR activation	2.26E+00	APOE, SCD, C3, MSR1 (includes EG:20288), IL1RN, LPL, CLU, CD14, IL6, GC

TLR7 agonist enhanced the therapeutic antitumor effects of GVAX therapy using irradiated autologous GM-CSF gene-transduced vaccine cells in both LLC and CT26 tumor-bearing mouse models with augmented pDC activation. These results showed that the combination of GVAX and imiquimod is an effective therapeutic strategy for cancer immunotherapy, and indicate that activated pDCs have a critical role in the GM-CSF–induced induction of antitumor immunity.

Materials and Methods

Mice

Five- to 10-week-old female immunocompetent C57/BL6N and BALB/cN mice were purchased from Charles River Laboratories Japan and housed in the animal maintenance facility at Kyushu University (Fukuoka, Japan). Type I IFN receptor knockout ($IFNAR^{-/-}$) mice were purchased from The Jackson Laboratory. All animal experiments were approved by the Committee of the Ethics on Animal Experiments in the Faculty of Medicine, Kyushu University. Mouse experiments were carried out at least twice to confirm results.

Tumor cell lines

LLC and CT26 cells were purchased from the American Type Culture Collection (ATCC) and passaged for 3 to 4 months after resuscitation. The mouse melanoma cell line (B16F10) was a kind gift from Dr. Shinji Okano (Kyushu University) and was validated as free from *Mycoplasma* infection; no other validations were performed. Both LLC and CT26 cells were validated as free from *Mycoplasma* infection. No other validations were performed; besides, the former were found as free from ectromelia virus. LLC and B16F10 cells were maintained in Dulbecco's Modified Eagle Medium (DMEM; Nakalai Tesque) supplemented with 10% heat-inactivated fetal bovine serum (FBS) and 1% antibiotic mixture (Nakalai Tesque). CT26 was maintained in RPMI-1640 (Nakalai Tesque) supplemented with 10% FBS and 1% antibiotic mixture.

Gene transduction with nontransmissible recombinant Sendai virus vectors

LLC, B16F10, or CT26 cells were infected with nontransmissible Sendai virus vectors encoding green fluorescence protein (GFP) or mouse GM-CSF (SeV/GFP or SeV/GM, respectively), which were prepared by DNAVEC Corp. (6), at the indicated multiplicity of infection (MOI) for 90 minutes (termed as LLC/SeV/GFP, LLC/SeV/GM, B16/SeV/GFP, B16/SeV/GM, or CT26/SeV/GM cells, respectively). They were cultured for 48 hours after viral gene transduction and used for following mouse studies.

Figure 2. GM-CSF–sensitized DCs elicited superior capacities to stimulate T-cell proliferation and to mobilize TAA-phagocytosed mature DCs into TDLNs. A, CFSE-labeled allogeneic MLR assay. Irradiated $CD11c^+$DCs from mice treated with indicated tumor challenge were mixed with CFSE-labeled allogeneic T cells. After 3 days of coculture, the proliferation rates of T cells were assessed by flow cytometric analysis. Representative histograms depict CFSE expression of allogeneic $CD4^+CD3^+$ or $CD8^+CD3^+$ T cells (left). Bar graphs, mean + SEM percentage of CFSE-diluted cells/total indicated T cells (right). B, representative histograms depict frequency distributions of MFI of CD80 or CD86 expression in $CD11c^+$ DCs from indicated mouse groups on day 2 or 4 after the tumor challenge (left). Bar graphs, mean + SEM of MFI of CD80 on DCs in TDLNs (right). C, representative dot plots show $PKH26^+CD11c^+$ cells gated by their FSC/SSC profiles in TDLNs or CLNs (left). Bar graphs, mean + SEM of percentage of $CD11c^+PKH26^+$ cells in TDLNs or CLNs (right). D, bar graphs, mean + SEM of MFI of CD86 expression levels in $PKH26^+CD11c^+$ cells (*, $P < 0.05$; ***, $P < 0.001$).

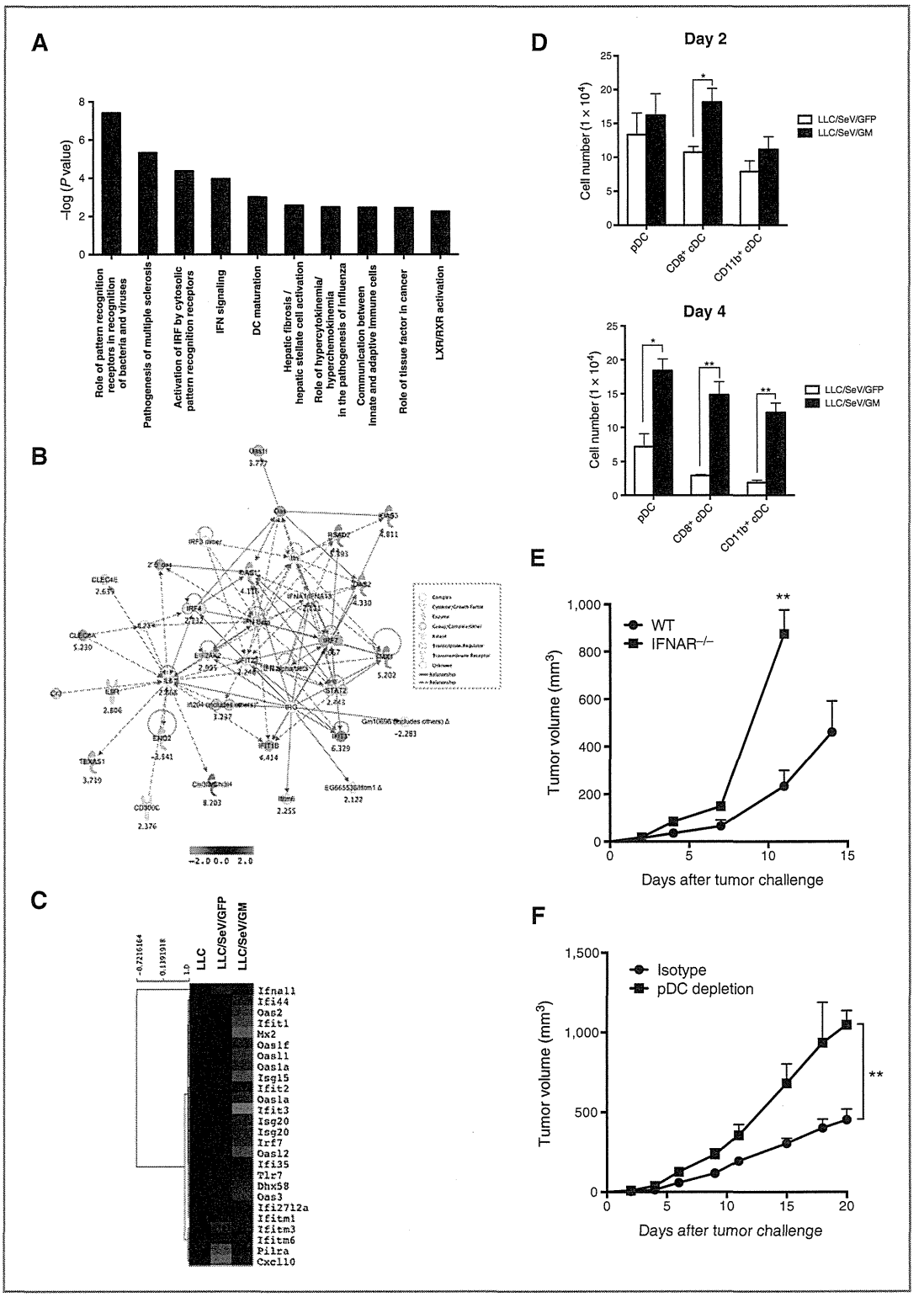
A
−log (P value)
Role of pattern recognition receptors in recognition of bacteria and viruses
Pathogenesis of multiple sclerosis
Activation of IRF by cytosolic pattern recognition receptors
IFN signaling
DC maturation
Hepatic fibrosis / hepatic stellate cell activation
Role of hypercytokinemia/ hyperchemokinemia in the pathogenesis of Influenza
Communication between innate and adaptive immune cells
Role of tissue factor in cancer
LXR/RXR activation
B
−2.0 0.0 2.0
C
LLC
LLC/SeV/GFP
LLC/SeV/GM
Ifna11
Ifi44
Oas2
Ifit1
Mx2
Oasl1f
Oasl1
Oasl1a
Isg15
Ifit2
Oasl1a
Ifit3
Isg20
Isg20
Irf7
Oasl2
Ifi35
Tlr7
Dhx58
Oas3
Ifi27l2a
Ifitm1
Ifitm3
Ifitm6
Pilra
Cxcl10
D
Day 2
Cell number (1 × 10^4)
LLC/SeV/GFP
LLC/SeV/GM
pDC
CD8+ cDC
CD11b+ cDC
Day 4
E
WT
IFNAR−/−
Tumor volume (mm3)
Days after tumor challenge
F
Isotype
pDC depletion
Tumor volume (mm3)
Days after tumor challenge